



Strål
säkerhets
myndigheten

Swedish Radiation Safety Authority

Research

Geophysical surveys on sub marine land- and rock slides and on alpine glaciers

2022:08

Authors: Per Holmlund and Martin Jakobsson,
Erik S. Mannerfelt, Matt O'Regan, Anton Wagner
and Elizabeth Weidner

Stockholm University

Report number: 2022:08

ISSN: 2000-0456

Available at: www.ssm.se

SSM perspective

Background

The future climate evolution and the impact it might have on a repository for radioactive waste is important when assessing the long-term safety. In a project funded by SSM (Holmlund et al. 2016), bathymetric data from the Southern Quark area between Sweden and Åland, provided by the Swedish Maritime Administration, were analysed, as well as terrestrial data from a glacial morphological mapping campaign. A broad range of landforms could be observed in these data and the overall glacial morphology pointed towards a powerful glacial impact involving an abundance of meltwater. Traces of mass wasting on the bottom of the deep trough through the Southern Quark were found. The genesis, timing and size of these deposits are important to resolve in order to assess their potential impact on nuclear facilities in the Forsmark area.

This study examined the bottom conditions in the Southern Quark, with a particular focus on indications from the previous study by Holmlund et al. (2016) on submarine mass wasting. Furthermore, in order to increase the understanding of the underlying processes that have shaped the glacial traces observed in the Southern Quark area, a study were performed on present glaciers in northern Sweden.

Results

The mass wasted rock debris affects an area >400 m wide of the seafloor in front of the steep wall that gave away. Rock slides on land occur regularly as a consequence of long-term rock disintegration from, for example, fluvial weathering on rather steep slopes (Abele, 1994). In the submarine environment, mass movements of sediments are common and may be triggered by mechanisms such as, for example, high sedimentation rates, glacial erosion, sea-level change and tectonic movements (Leynaud et al., 2009). The occurrence of submarine rock slides is, however, much less documented and therefore also less known. In general, the survey of the area shows strong bottom currents and a very dynamic oceanography in the investigated area today and it is likely that the area were equally dynamic during the deglaciation. Beneath the top sediment layers are buried channels that are probably derived from deglaciation and a plentiful supply of melt water. Thus, a plausible time when the rock slide could have occurred is during the deglaciation, but the genesis of the rock slide remains unknown.

The results from the present glaciers in northern Sweden show clearly the effect of the thermal conditions and they also show both that the boundary between basal frozen and basal melting conditions is sharp and it may move its position over time due to changes in ice thickness and climate change. In an analogue to basal conditions beneath the Weichselian ice sheet there may have been short distances between high erosion rates and hardly no erosion at all. The transition zone between these two different environments is not stable over time and is rather expected to have varied in its location.

Relevance

The project intends to increase the knowledge regarding the significance of the marine collapse structures outside Forsmark (Southern Quark). Knowledge of any post-glacial earthquakes (PGF) that have or may occur near a final repository for spent nuclear fuel is of high interest to SSM since large earthquakes can induce secondary fault movements in the repository volume which could damage deposited canisters. In addition, the identification of stronger PGFs would mean that SKB's assumed earthquake frequency needs to be improved.

Future potential erosion during several glacial cycles are an important climate related process to consider for a repository of spent nuclear fuel since a lowering of the bedrock surface can affect the assessment of future human intrusion as well as the assessment of radionuclide transport. The study of Scandinavian alpine glaciers aims to improve our understanding of ice behaviour and sharp unconformities in erosion rates.

Need for further research

A geohazard from large mass movements on the seafloor, whether of rocks or sediments, is the generation of a tsunami (Ioualalen et al., 2010). A numerical simulation of a potential tsunami caused by the identified rock slide in the Southern Quark comprises one of several topics for follow-up studies that could be made based on the material acquired in this study, as it may have bearing on present nuclear facilities in the Forsmark area.

Project information

Contact person SSM: Carl-Henrik Pettersson

Reference: SSM 2016-644/ 3030045-30



Strål
säkerhets
myndigheten

Swedish Radiation Safety Authority

Authors: Per Holmlund and Martin Jakobsson, Erik S. Mannerfelt, Matt O'Regan,
Anton Wagner and Elizabeth Weidner
Stockholm University

2022:08

Geophysical surveys on sub marine
land- and rock slides and on alpine
glaciers

Date: June 2022

Report number: 2022:08 ISSN: 2000-0456

Available at www.stralsakerhetsmyndigheten.se

This report concerns a study which has been conducted for the Swedish Radiation Safety Authority, SSM. The conclusions and viewpoints presented in the report are those of the author/authors and do not necessarily coincide with those of the SSM.

Geophysical surveys on sub marine land- and rock slides and on alpine glaciers

*Per Holmlund and Martin Jakobsson, Erik S, Mannerfelt, Matt
O'Regan, and Elizabeth Weidner, Stockholm University*

Contents

Summary	1
Sammanfattning	3
1. Introduction	5
2. Survey with Stockholm University RV Electra	6
2.1. Geology of the survey area	8
2.2. Expedition participants.....	10
3. Survey on glaciers in Northern Sweden	11
3.1. The thermal structure within the ice	13
4. Methods - marine mapping and coring	16
4.1. Geophysical mapping with RV Electra	16
4.1.1. Equipment overview	16
4.1.2. Multibeam echo-sounder	17
4.1.3. Sub-bottom profiler	18
4.1.4. Position, heading and attitude	18
4.1.5. Midwater sonar	18
4.1.6. Acoustic Doppler Current Profiler (ADCP)	19
4.1.7. Water properties (Sound speed, temperature, salinity).....	19
4.1.8. Acoustic synchronization unit	19
4.2. Sediment coring and temperature logging	20
4.2.1. Piston/gravity corer and coring winch.....	20
4.2.2. Temperature logging.....	24
4.2.3. Core Logging and Description	27
4.2.4. Bottom filming	28
5. Methods - geophysical mapping in Swedish Lapland	28
5.1.1. Radar soundings.....	28
5.1.2. Photography and photogrammetry	29
5.1.3. Data processing	31
6. Results - marine mapping and coring	32
6.1. Geophysical mapping from RV Electra	32
6.1.1. Multibeam bathymetry	32
6.1.2. Midwater	37
6.1.3. Sub-bottom profiling.....	42
6.2. Sediment coring	45
6.2.1. Core Lithology.....	46
6.2.2. Temperature logging.....	53
7. Results - Geophysical mapping in Swedish Lapland	55
8. Discussion and recommendation for further study	58
9. Conclusions	60
References	61
Appendix 1: deliverables	65
Appendix 2: Core Logs	66

Summary

A future glaciation is expected to have a major impact on a final repository for nuclear waste. The important question is how big the impact could be. In a project funded by SSM (Holmlund et al. 2016), bathymetric data from the Southern Quark area between Sweden and Åland, provided by the Swedish Maritime Administration, were analyzed, as well as terrestrial data from a glacial morphological mapping campaign. A broad range of landforms could be observed in these data and the overall glacial morphology pointed towards a powerful glacial impact involving an abundance of meltwater. Traces of mass wasting on the bottom of the deep trough through the Southern Quark were found. Given the large variations in ice load on Earth's crust that occur during a glaciation, it is reasonable to imagine periods of significant tectonic activity with earthquakes as a result.

In this study, we further examined the bottom conditions in the Southern Quark, with a particular focus on indications from our pre-studies on submarine mass wasting. One of the identified rock slides is very large and has been mapped in detail with Stockholm University's research vessel *RV Electra*. The field work included collection of sediment cores, temperature measurements in the uppermost sediments, oceanographic stations and geophysical mapping of the seafloor and unconsolidated sediments with multibeam sonar and sub-bottom profiler. In addition, acoustic data were collected of the water column using *RV Electra's* "fish" echo sounder to investigate the occurrence of gas seeps from the seabed. The field work was carried out in August 2017. The large mass wasting of rocks may be indicative of post-glacial tectonic movements in the area. In addition, concave topographic features were mapped that also may indicate movements in the crust following the deglaciation. These and the mass wasting have so far not been possible to date using the retrieved sediment cores, although preliminary attempts to date key lithologic boundaries in the sediment cores, and hence age-calibrate the sub-bottom data are underway as part of a Master's thesis at IGV. In general, the survey of the area shows strong bottom currents and a very dynamic oceanography in the area today, that does not appear to be as active or vigorous during the earlier part of the Holocene. Beneath the uppermost sediment layers are buried channels that were probably formed during the deglaciation from a plentiful supply of melt water. Relatively large variations in bottom water temperatures affect the temperature of the upper sediments, which resulted in a geothermal gradient not being possible to determine from our measurements.

To understand the underlying processes that have shaped the glacial traces that we see in the Southern Quark area, we have also studied the temperature distribution in recent glaciers. The temperature at the bottom and in the ice-body itself provide the basis for which landforms are formed by a retreating glacier or ice sheet. We performed radar measurements from helicopters to map the glaciers' temperature distribution and we carried out photogrammetric measurements and mappings of the areas of the glaciers' margins. A bottom-melting glacier erodes the substrate while a bottom-frozen glacier preserves the substrate. Glaciers with spatial variations in bottom temperature are given

a range of landforms that help us draw conclusions on how an upcoming glaciation may affect the landscape around Forsmark. An important piece of the puzzle regarding how the temperature distribution will look like is how the glaciation process develops, from a mountain glaciation to a full-scale ice sheet over Scandinavia. Sharp boundaries may exist between the areas underneath the ice sheet where the base is frozen to the ground and where it is not, but it is not certain where these boundaries will end up. The difference is negligible erosion underneath the base of the ice, or several tens of meters of erosion. But a bottom-melting ice can also accumulate moraine material beneath it and the sliding can take place in underlying sediment layers implying that the real situation is very complex.

Sammanfattning

En framtida glaciation kan förväntas ha stor inverkan på ett slutförvar för kärnavfall. Den viktiga frågan är hur stor inverkan kan bli. I ett projekt som finansierades av SSM (Holmlund m f. 2016) analyserades batymetriska data från Sjöfartsverket över Södra Kvarken mellan Åland och Sveriges fastland, samt terrestra data från en glacialmorfologisk kartering där en stor rikedom av landformer kunde observeras. Spåren vittnade om en kraftfull glacial påverkan där rikligt med smältvatten förekommit. I djuprännan genom Södra Kvarken syntes även spår av ras på botten. Vid de stora variationer i trycklast som sker under en glaciation är det rimligt att tänka sig perioder med betydande tektonisk aktivitet med jordskalv som följd.

I denna studie har vi undersökt bottenförhållandena i Södra Kvarken, med ett särskilt fokus på indikationer ifrån våra förstudier på submarina ras. Ett av rasen är mycket stort och har karterats i detalj med Stockholms universitets forskningsfartyg RV *Electra*. Fältarbetena omfattade insamling av sedimentkärnor, temperaturmätningar i de översta bottensedimenten, oceanografiska stationer och geofysisk kartläggning av botten och de lösa bottensedimenten med multistråligt och penetrerande ekolod. I tillägg insamlades ekolodsdata över vattenkolumnen med RV *Electras* fiskekolod för att undersöka förekomsten av gasflöden från botten och skiktningar i vattnet. Arbetena utfördes under augusti månad 2017. Rasen kan vara indikationer på postglacial tektoniska rörelser i området. I tillägg visade kartläggningen på en konkav struktur i havsbotten vilken kan vara ett tecken på postglacial tektonik. Dessa samt rasen har ännu inte kunnat daterats med hjälp av de sedimentkärnor som togs. Generellt visar kartläggningen av området på starka bottenströmmar och en mycket dynamisk oceanografi i området i dag. Under de översta sedimentlagren finns begravda kanaler som troligen härrör från deglaciationen och en riklig förekomst av smältvatten. Relativt stora variationer i bottenvattentemperaturer påverkar temperaturen i de översta sedimenten vilket resulterat i att en geotermal gradient inte kunnat bestämmas från våra mätningar.

För att förstå de bakomliggande processer som utformat de glaciala spår som vi ser i Södra Kvarkenområdet har vi även studerat temperaturfördelningen i recenta glaciärer. Temperaturen vid botten och i själva iskroppen ger förutsättningen till vilka landformer som bildas vid en retirerande front. Vi har utfört radarmätningar från helikopter för att kartlägga glaciärernas temperaturfördelning och vi har utfört fotogrammetriska mätningar och karteringar av glaciärernas frontområden. En bottensmältande glaciär eroderar underlaget medan en bottenfrusen glaciär bevarar underlaget. I glaciärer med rumsliga variationer i botten temperatur fås en flora av landformer som hjälper oss att dra slutsatser om hur en kommande glaciation kan komma att påverka landskapet kring Forsmark. En viktig pusselbit i hur temperaturfördelningen kommer att se ut är hur glaciationsförloppet utvecklas, från en montanglaciation till ett fullskaligt istäcke över Skandinavien. Skarpa gränser kan förekomma mellan bottenfrusna och bottensmältande partier men det är inte givet var dessa gränser kommer att hamna. Skillnaden är försumbar erosion, eller flera tiotals meter i erosion. Men en bottensmältande is kan även

ackumulera moränmaterial under sig och glidningen kan ske i underliggande sedimentlager så den verkliga situationen är mycket komplex.

1. Introduction

An ice sheet affects its substratum in many different ways. The glacier erodes, groundwater flow is affected (Lemieux & Sudicky, 2011), tectonic movement take place due to variation in ice-load on the crust (Steffen et al., 2014), landforms are shaped and the ice sheet distributes till and sediments (Dowdeswell et al., 2016). Crucial forcing parameters are the temperature distribution within the ice and the speed of the changes in overburden pressure. The last glaciations were characterized by a successive cooling of the climate until it reached a maximum (Ehlers et al., 2018). During most of the Quaternary glaciations, ice sheets covered the high mountains in northern Europe and Scandinavia and expanded beyond the high terrain into lowland areas to occupy parts of the marine realm (Hughes et al., 2016). During the Late Weichselian glaciation, a.k.a. Last Glacial Maximum, permafrost was formed in inland Sweden while the ice sheet grew thicker and slowly advanced towards the Gulf of Bothnia. However, the lake/sea bed in this area was apparently not frozen allowing basal sliding and/or sediment sliding beneath the ice. An ice stream was established heading south along the Gulf of Bothnia and the Baltic Sea with relatively high ice velocities and ice fluxes (Greenwood et al., 2017). The underlying bedrock was depressed and the potential for high rates of glacial erosion was significant. During the deglaciation, the ice stream remained and, as a consequence, the recession through the Gulf of Bothnia was quick due to the efficient ice flux (Greenwood et al., 2017). The process of initial ice load and final unload was therefore fast and tectonic movements resulting in earth quakes and small rock displacements were probably usual events. Evidence of tectonics and major earth quakes following from unloading of the retreating Late Weichselian Ice Sheet have been found in several areas of Scandinavia (Jakobsson et al., 2014; Lagerbäck & Sundh, 2008). During the last glaciation we had two major advances and corresponding recessions.

In the vicinity of Forsmark there are strong gradients in observed traces of glacial erosion. Further inland in Uppland, there are clear indications of glacial erosion, but erosional rates are unclear. In the Åland Sea, east of Forsmark, we have clear evidences of glacier erosion and typical features of glacier landscape modulation such as *roche moutonnées*, i.e. rock formations created by an overrunning glacier, and pure rock displacements. The narrow passage of Åland Sea separating Uppland and Åland Archipelago, where the ice stream flowed through, is nearly 300 meters deep (Jakobsson et al., 2019) and now covered with >50 m sediment and till in the deeper parts. The seafloor bathymetry is rough with steep >150 m high walls. Pre-investigations to this project indicated substantial mass wasting at the seafloor from analyses of bathymetric data made available by the Swedish Maritime Administration. However, no detailed geophysical mapping of the seafloor sediment or sediment cores existed preventing further investigations.

In this project we have improved the bathymetric portrayal of the area significantly by acquisition of additional high-resolution multibeam bathymetry, we have carried our sub-bottom profiling to image the sediment stratigraphy and retrieved sediment cores using a corer equipped with temperature loggers. Furthermore, a split beam fish echo sounder was used

to gather information of the water column and detect if seeps existed in the area. The marine surveys were performed in August 2017 with Stockholm University's Research Vessel *Electra*. In addition, recent Scandinavian alpine glaciers have been analysed concerning the link between thermal structure in the ice and proglacial landforms. The aim of this study is to improve our understanding of ice behaviour and sharp unconformities in erosion rates.

2. Survey with Stockholm University RV *Electra*

Expedition EL17-IGV04 was focused on marine geophysical mapping and coring in Södra Kvarken located between Sweden and Åland (Fig. 1). The objective was to map the seafloor for submarine slides and signs of tectonic movements following the retreat of the Scandinavian Ice Sheet (SIS). The survey constituted the marine component of a project supported by the Swedish Radiation Safety Authority (Strålsäkerhetsmyndigheten) aiming to gather information about glacial erosion and potential postglacial tectonic movements in the vicinity of Forsmark, located approximately 140 km north of Stockholm on the Swedish east coast. Forsmark is the location of a nuclear power plant and was selected in 2009 by the Swedish Nuclear Fuel and Waste Management Co (SKB) to become a Spent Fuel Repository. In 2011, SKB submitted the applications to build the repository in Forsmark.

RV *Electra* was based in Grisslehamn on the northern Vaddö Island during the field work days (Fig. 2). The survey program began Sunday 6 August and was intended to continue until Friday 11 August. However, during the third survey day, RV *Electra* hit a 2.3 m deep uncharted shoal located on the official navigational chart outside of the 15 m depth contour east of Understen (Fig. 3). The hull was damaged at the stern where the ice knife is located and some meters aft of the ice knife on the starboard side. Two small holes in welding seams opened, one 2 cm long and the other 5 cm long. Following inspection and temporary repair made by divers, RV *Electra* had to go to Tenö Shipyard in Vaxholm for proper repair of the damage. The repair was made during 10-11 August, and the survey was continued from midday 13 August and ended 17 August.

The fieldwork with RV *Electra* consisted of geological coring, oceanographic stations, in situ sediment temperature logging and geophysical mapping including multibeam bathymetry, sub-bottom profiling, and midwater sonar. Participants in the survey are listed in Table 1. After an initial reconnaissance mapping, the coring program commenced, which subsequently was alternated by more geophysical mapping. The oceanographic stations were comprised of conductivity, temperature and depth (CTD) profiles. This report consists of a brief description and initial assessment of the geology of the survey area, description of the applied methods and summary of the collected data. Permission to carry out geophysical mapping in Södra Kvarken was granted by the Swedish Armed Forces (Försvarsmakten, permit FM2017-15117:3). The collected mapping data have been granted permission for public release by the Swedish Maritime Administration. In addition to the presented results

in this report, deliverables from the marine surveys are comprised of the geophysical mapping data and the parameters measured on retrieved sediment cores which will form the basis for a Master's project at IGV in 2021-2022, and further studies. The acquired multibeam bathymetry from Södra Kvarken have been used in a study of the Baltic Sea bathymetry since the complex seafloor morphology in this area influences the connection between the Bothnian Sea and Northern Baltic Proper across Åland Sea (Jakobsson et al., 2019).

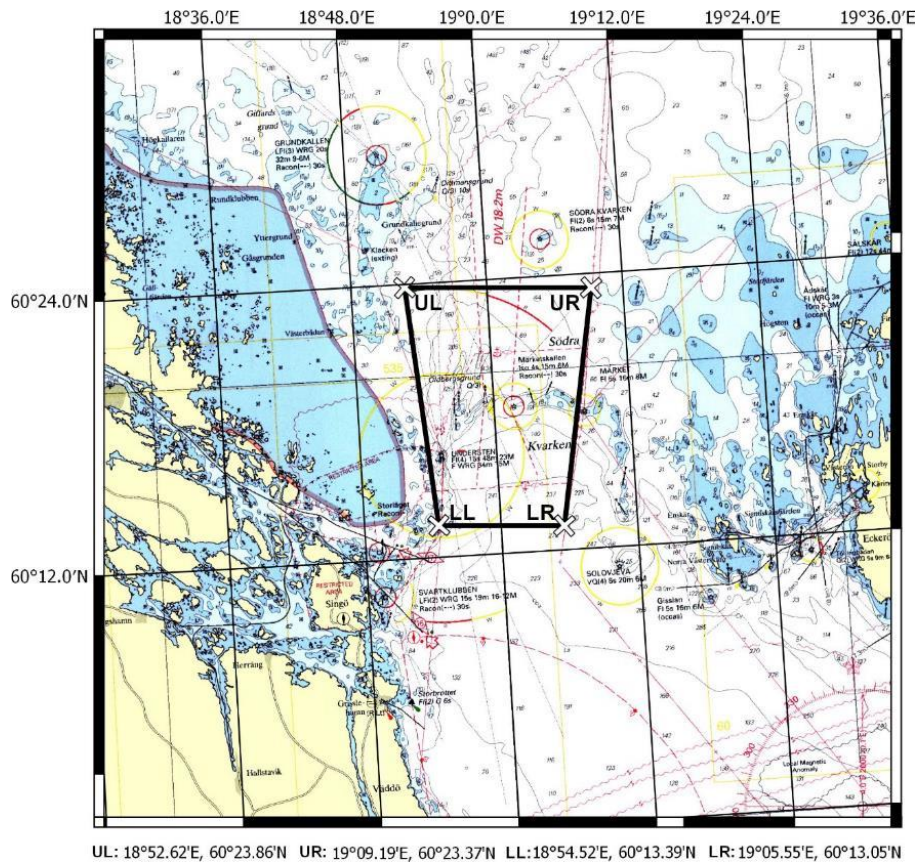


Figure 1. Survey area in Södra Kvarken between Sweden and Åland. The area for which survey permit (Försvarsmakten, permit FM2017-15117:3) was granted is shown with a black box. The coordinates of the corners are listed below the map in WGS 84.



Figure 2. RV Electra at the dock in Grisslehamn, northern Väddö.



Figure 3. Screen dump of the ECDIS chart at the location where RV Electra hit the shoal east of Understen. Note that the actual collision occurred well outside of the 15 m depth contour. The shoal will be reported to the Swedish Maritime Administration.

2.1. Geology of the survey area

The general bedrock composition of the Baltic Sea seafloor has been mapped using geophysical methods and geological coring and drilling (Flodén, 1992; Flodén et al., 1980; Tuuling et al., 1997; Winterhalter et al., 1981). Applied geophysical mapping methods included, for example, acquisition of marine

seismic reflection and refraction profiles and gravity as well as magnetic surveys. A summary of the pre-Quaternary geological history of the Baltic Sea is provided by Beckholmen and Tirén (2009).

The retreat dynamics of the SIS during the last deglaciation of the area today occupied by the Baltic Sea is poorly known. This results from few available sediment cores containing deglacial records and a near complete lack of available high-resolution seafloor mapping data permitting analyses of submarine glacial landforms. Geological information from the shores surrounding the Baltic Sea have instead been used to infer the retreat dynamics (Kleman et al., 1997; Lundqvist, 2004, 2007) along with the sparse high-resolution mapping information available (Andrén et al., 2011). However, recent analyses of multibeam mapped areas in the Gulf of Bothnia have provided new insights, suggesting complex retreat dynamics involving considerable input of meltwater and rapid break-up over large sectors north of Åland (Greenwood et al., 2016a; Greenwood et al., 2017; Greenwood et al., 2016b; Jakobsson et al., 2016). A review of the deglacial to post-glacial development of the Baltic Sea is provided by Björck (1995) and is also included in Andrén et al. (2011). The Integrated Ocean Drilling Program (IODP) expedition 347 recovered sediments in 2013 from nine coring sites spread out from Bornholm Basin in the south to the Ångermanälven River estuary in the north (Andrén et al., 2015). The survey area in Södra Kvarken is located at the boundary between different bedrock (Fig. 4).

An approximately 5 km wide belt of post-Jotnian diabase (shown as dolerite on Fig. 4) extends from Märketskallen in the east on available maps, e.g. on maps from Swedish Geological Survey. The bedrock to the south is mapped as Jotnian sandstone, conglomerate, siltstone and shale. Granitic rocks dominate the bedrock west of the diabase, while the seafloor north of the diabase appears as unknown on available maps. Understen Islands are shown as being comprised of ultrabasic rocks (Fig. 4).

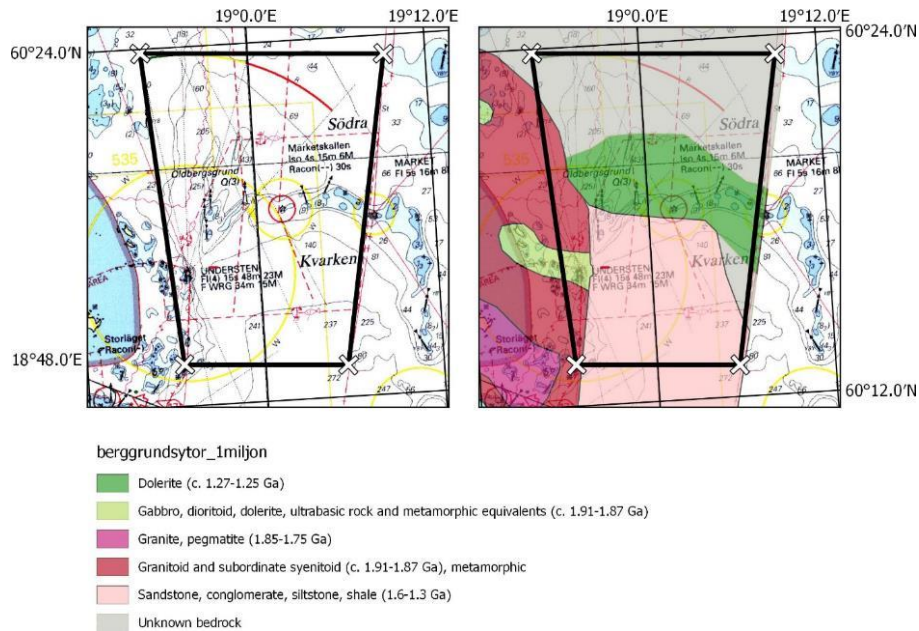


Figure 4. The survey area in Södra Kvarken. The navigational chart by the Swedish Maritime Administration is shown in the left map and general bedrock composition is shown in the map to the right. The geological information is extracted from the Geodataportal (<https://www.geodata.se/>) and is based on information from the Swedish Geological Survey.

Multibeam bathymetry covering parts of Södra Kvarken was rented from the Swedish Maritime Administration (SMA) during the initial phase of the project for planning purposes. Their bathymetric data show that the seafloor in Södra Kvarken is characterized by a dramatic underwater topography with near vertical scarps rising, in places, more than 200 m. The deepest depth of 274 m is recorded in the southeast corner of the survey area. The belt of diabase closely coincides with a set of ridges rising in places >100 m from the surrounding seafloor and striking NNE. The ridges have sharp, near vertical walls, on their western sides and slopes between 10 and 15° on their eastern sides. Furthermore, the multibeam bathymetry from SMA show signs of severe bottom current erosion along the bedrock ridges and hinted at the existence of mass movements in several places. It proved to be more cost-efficient to re-survey the area of interest in Södra Kvarken in this project than to continue and lease data from SMA, and this permitted also collections of additional geophysical mapping data than bathymetry. Since the seafloor was bathymetrically mapped in detail during this project, it will be further described in the results section.

2.2. Expedition participants

Expedition EL17-IGV04 was divided into two parts separated by the repair of RV *Electra* at Tenö shipyard. The scientific crew remained the same on both parts, but the ship crew was partly changed. The expedition participants are listed in Table 1.

Table 1. Participants in expedition EL17-IGV04.

Name	Main Role	Organization
Scientific crew		
Draupnir Einarsson	Coring	Department of Geological Sciences, Stockholm University
Björn Eriksson	Geophysical mapping/IT	Department of Geological Sciences, Stockholm University
Sarah Greenwood	Participated the last day in order to plan for following Expedition EL17-IGV05.	Department of Geological Sciences, Stockholm University
Martin Jakobsson	Project Leader/Geophysical mapping/Coring	Department of Geological Sciences, Stockholm University
Matt O'Regan	Coring/heat flow	Department of Geological Sciences, Stockholm University
Aron Varhelyi	Coring/Student	Department of Geological Sciences, Stockholm University
Elizabeth Weidner	Geophysical mapping/Student	Center for Coastal and Ocean Mapping (CCOM), University of New Hampshire, USA
Crew		
Susann Eriksson	(Participated part one)	Baltic Sea Centre, Stockholm University
Mattias Murphy		Baltic Sea Centre, Stockholm University
Thomas Strömsnäs	Captain	Baltic Sea Centre, Stockholm University
Carl-Magnus Wiltén	(Participated part two)	Baltic Sea Centre, Stockholm University

3. Survey on glaciers in Northern Sweden

The temperature distribution within a glacier and at its substratum governs the way the glacier moves and how it may affect the bed. During the Weichselian glaciation we might have had melting conditions beneath the ice in the Kvarken area (Holmlund et al. 2016). But it is as evident that we have had frozen conditions at least on parts of both Åland and Uppland and in between a Baltic Ice Stream (Holmlund and Fastook 1993, Holmlund et al 2016). The border between frozen and thawing base was evolving over time. If a bed at the melting point freezes the substratum will freeze on to the ice and cause plucking. On the Swedish side of Kvarken there are evidences of plucking of rock slabs probably at the very end of the glaciation when the ice thins but keeps its low temperature (Holmlund et al 2016). Temperature conditions can change over time due to long term climatic influence, by thickness changes in the ice and by dynamic changes such as sudden shifts in path way of ice streams. In this project we have focused on small mountain glaciers and study how their flux rates and erosion rates change with changing temperatures.

Glaciers are by definition very good climate indicators as their size and form are determined by the climate. The exponential relation between thickness and ice flow causes strong responses also to small climatic changes. However, the response time of Swedish subarctic glaciers are typically 50-100 years so observed length changes is a result of not only present, but also the last century climate filtered and diffused through the glacier. The Swedish glaciers have a polythermal temperature regime, meaning that they are in part temperate and in part of a cold polar type (Holmlund and Eriksson 1989, Pettersson et al. 2003). The relation between these two regimes differs due to local climate effects. In the simplest case the glaciers are temperate in their accumulation area and more or less cold in their lower parts. But in permafrost regions the temperature regime is complicated by ice cored moraines and perennial snow fields physically linked to the glaciers and thus influencing their way of responding to the climate (Holmlund 1998).

The relation between temperate and subfreezing ice varies with local climate conditions. In dry areas the proportion of cold ice is higher compared to the corresponding proportion in wetter areas. The proglacial areas typically have flutings, and sedimentary piles including both till and sediments that have been smeared out during past advances. Ice cored moraines in northern Sweden are common features especially in the eastern side of the mountains which has a locally continental climate (Ångström 1980). Finally, there is normally a set of frontal moraines indicating former maximum extensions. However, there are exceptions from this general scheme. Some glaciers show almost no glacial landforms in their proglacial area, and some have almost no frontal moraines.

It is obvious that the way glacier advance their frontal position is not uniform, but unfortunately only few glaciers in Sweden have advanced over the last 100 years and none of them have made any major advance. So, an important issue is how these polythermal glaciers advance their frontal positions. The glaciers are frozen to their beds in the frontal zone. By ice thickening, the stresses may cause warming and at a point the glacier start to slide over its substratum. But other processes may also act, such as icing in front of the glacier allowing it to advance by internal deformation. The latter process would allow fragile landforms to survive underneath the advancing front. Still there are other sites where the glacier seems to have advanced more violently leaving no traces of past landforms, a surge like behavior.

The survey on glaciers in Northern Sweden describes four different glaciers physically and make an attempt to conclude why their responses to climate wiggles differ. The glaciers are Storglaciären, Mårmaglaciären, Rabots glacier and Mikkaglaciären (Fig. 5). These glaciers were selected based on access of useful data and on their different response to climate change. The glacier survey have been conducted by Prof. Per Holmlund, and Erik Schytt Holmlund presently a master student at UNIS, Svalbard. Four field campaigns were conducted in April 2017 and in August 2017, 2018 and 2019.

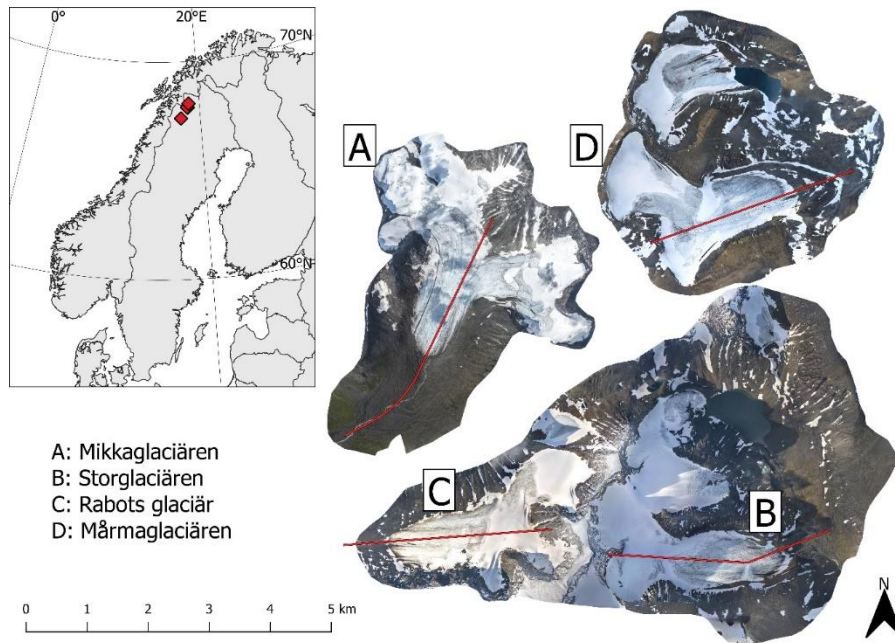


Figure 5. Location map

3.1. The thermal structure within the ice

The pattern of the temperature distribution within the ice is given by the pattern of snow accumulation, the rate of mass turnover and the air temperature (Pettersson et al. 2003). In the wintertime the surface of the glacier is cooled to a certain degree and a certain depth. In the spring when melting occurs, meltwater penetrates the snow pack and efficiently raise the temperature to the melting point by energy release from refreezing meltwater. In the accumulation area of a glacier this process will also warm up past years snow, so-called firn. Ice surfaces within and below the accumulated snow will impede the meltwater from further vertical penetration. Instead the meltwater will flow horizontally or refreeze at the ice surface. The cooling from the winter thus remains and forms over time a layer below which the temperatures are below the freezing point. In areas with low mass turn over, the thickness of this frozen layer is large, and in glaciers with a high rate of mass turn over this layer becomes thinner. Typical values for the frost depth in Swedish glaciers is 80 m in dry areas and 10-20 m in wetter areas. On glaciers originating from several cirques the thermal conditions can show very large spatial variability.

If a polythermal glacier thins its average temperature will decrease (Pettersson et al. 2003). A small glacier may freeze on to the substrata, which prevents it from sliding. The glacier can thus become steeper by this process, but it will at the same time hinder sufficient mass to be transported to the front. In a case of a shift to a more favorable climate for glaciers a small steep glacier can reach the melting point at the base and thus make a dramatic quick advance of its front position.

Glaciers in dry environments may become climatologically dead, but stay as a more or less extent ice field for a long time. The temperature at the base of such an glacier/ice field will be low due to the lack of water penetration and to the relatively low annual temperatures in the Swedish mountains.

The topography is very important both for the mass balance and the temperature distribution of a glacier. A steep head wall will provide the glacier with sufficient snow to allow a secure net income of mass and it will also provide a sufficiently deep snow/firn layer that ice will be formed at the pressure melting point. If there is no headwall or a gap in the headwall, much less snow will be accumulated and ice temperatures and thus ice velocities will be low.

In permafrost regions moraines often become ice cored. But, glaciers in a cold dry environment must not necessarily have ice cored moraines as moraine forming processes are to a large extent dependent on access of debris on the ice, such as rock falls from mountain sides. Glaciers formed like ice caps must not necessarily form large frontal moraines.

Moraine systems in front of glaciers describe a history of past climate changes, primarily cold events. A combination of summer melting and winter snow accumulation governs the size of glaciers, and local differences in for example topography may influence the way they respond to a given climate signal. Today all glaciers in Sweden are retreating due to a warmer climate and the precipitation increase is not sufficient to compensate for the increased melting. The size and shape of a glacier is governed by the climate and the climate signal is filtered through the glacier and determines its extension. This means that different glaciers may respond in different ways and with significantly different response time and magnitude of change. The Little Ice Age (LIA) terminated around 1910 in Northern Sweden (Holmlund 1993, Holmlund and Holmlund 2019) and glaciers reached extensions normally 97-100% of their Holocene maximum. During the course of the successive decade they lost 30-90% of their mass and some glaciers vanished completely. The way they respond is unique for each glacier, but what are the physical reasons for these differences?

Front moraines describe past advanced positions caused by cold climate. In Sweden, it is not unusual to find 4-8 moraines and at some locations more than 10. These moraines are often clustered within a relatively short distance meaning that the glacier has reached more or less the same extension during all Holocene cold events. At some locations there are bedrock or ice cored moraine obstacles preventing further advance, but at most locations there are no obvious reason why the glacier advance have stopped. The shape of the glacier and its location and orientation in relation to surrounding mountains may give semi stable extensions, but there are some sites where there are no observable physical settings that may restrict a further advance, except for climate. But if the climate is the only restricting force governing glacier size it implies that all Holocene cold events have been equally cold, had equally rate of precipitation and equal duration which is not very likely to be true.

In the High Arctic glacier surges are common phenomena where the physical conditions in the glacier makes it unable to transport sufficient ice mass from the upper part to the glacier tongue (Dowdeswell et al. 1995; Raymond, 1987). The cause of a surge is linked to the internal thermal distribution within the ice. The lower part of the glacier is thin and at below freezing point temperatures and also frozen to the bed. This cause the accumulation area to grow in thickness over time until it is too thick and too steep and it collapses in a surge-like behaviour due to rapidly increased internal deformation and basal sliding. This cause the accumulation area to thin and the glacier front makes a dramatic advance (0.1-10 km) over some months or a year. Such an advance is followed by a quiescent phase when the tongue thins, cools and starts retreating, while the accumulation area slowly grows again until the same story happens again. The frequency of surges varies from tens of years up to several hundred years.

On Svalbard there are examples of surges of different kinds and expressions (Farnsworth et al. 2016; Sevestre and Benn 2015), not only classical version influencing the entire glacier but also partial surges. An additional process that may cause surge like advance is related to the thickening of a glacier or an ice/snow field. If such a thickening occurs, it may reach a point when the basal temperature reaches the pressure melting point and the glacier advances fast and prominent. All these types of fast advances have in common that they leave deposit moraine features on the ground. The fast advance may cause glacier cracking in a chaotic manner also at the base, forming zig-zag patterns of moraines or eskers (Concertina eskers). If the sliding part of the ice flow terminates after the advance the morainic features remains undisturbed until they get exposed by deglaciation. Also other landforms and overridden front moraines may tell how the glacier once advanced.

In Sweden there have been no observations of surging glaciers, but observations have been made of small glaciers with a collapse like behaviour after some years of mass build up. A good example is a nameless glacier on the western side of Mietjevagge in the Sulitelma massif which has been documented with photos since the mid 1970s with at least three collapses but the data is unpublished. Also, there are several glaciers with pre requisites for a surge behaviour and where it is possible that surges have occurred in the past. A surge is not decoupled from climatic wiggles but it governs how the glacier change its shape and how extensive it gets once it advance (Sevestre and Benn 2015). If the climate is favourable for glacier growth after the surge the glacier may instead of retreating grow in thickness. If so it is possible that the most typical surge indicative landforms may get destroyed by the glacier.

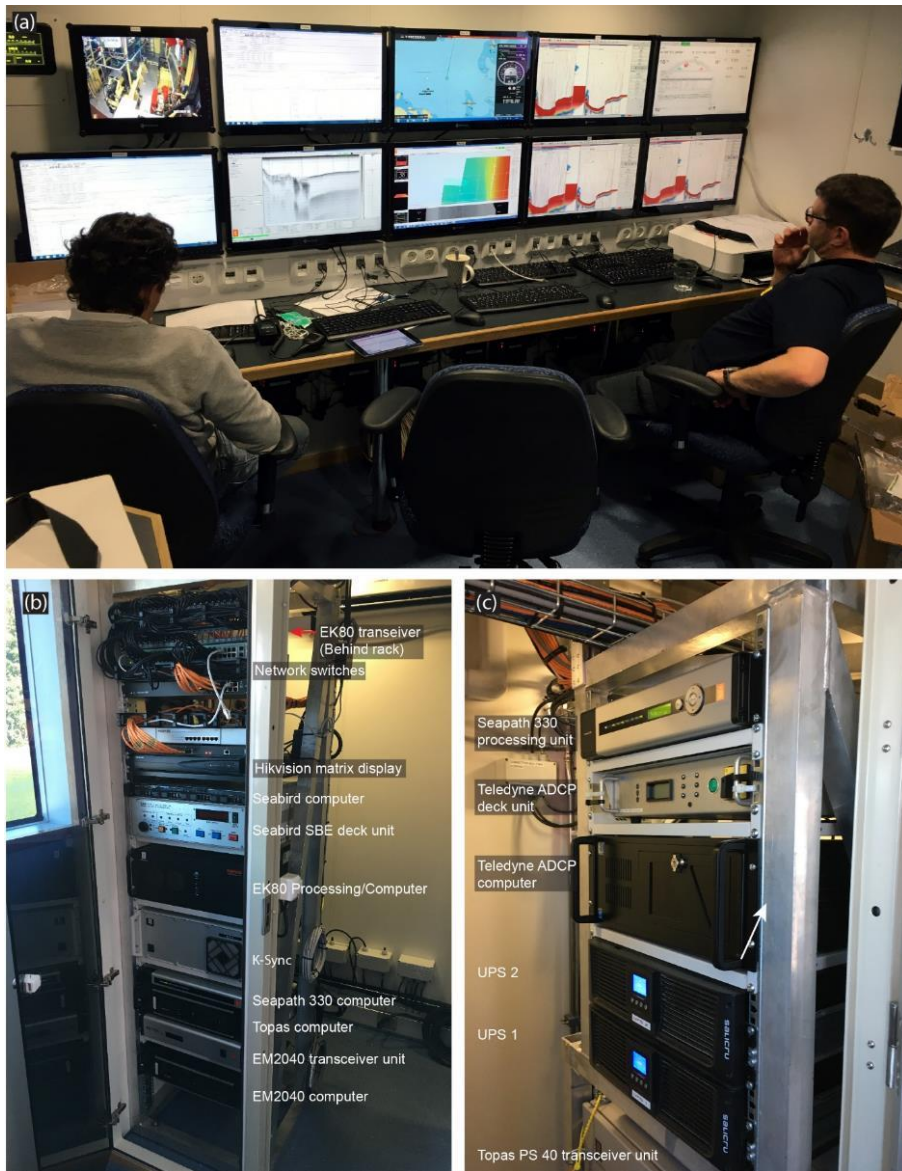


Figure 7. The dedicated “apparatus room” on RV Electra. **(a)** Nine wall-mounted screens on the aft wall of the apparatus room are connected to a display matrix system permitting switching between all computers controlling sonars, Seapath navigation/attitude system and CTD. USB input for keyboard and mouse are mounted below the screens. This makes it possible to decide which system to display on any of the nine included screens, the tenth screen (upper left) is connected to a camera system. The display matrix system is also extended to the bridge, permitting control and display of the sonars systems on the bridge. **(b,c)** Rack-mounts of all units belonging to the sonar systems, Seapath navigation, and CTD. The rack are installed in a cooled enclosed part of the apparatus room.

4.1.2. Multibeam echo-sounder

RV *Electra* has a hull-mounted Kongsberg EM2040 $0.4^{\circ} \times 0.7^{\circ}$, 200-400 kHz, multibeam echo-sounder. The along ship transmit 0.4° transducer array is (L×W) 727×142 mm and the across ship 0.7° receive transducer array is

407×142 mm. The echo-sounder is operated using Kongsberg's Seafloor Operation System (SIS), version 4.3.2 (Build 31, DBVersion 30.0). The EM2040 includes the capability of logging acoustic data of the water column. It has a maximum depth capacity of 600 m and the swath width varies depending on used frequency, water properties and bottom types. It usually ranges between covering about 4 and 6 times the water depth.

4.1.3. Sub-bottom profiler

A Kongsberg Topas PS40, 24ch, parametric sub-bottom profiler is hull-mounted in RV *Electra*. The transmit transducer is (L×W) 830×540 mm and the hydrophone unit is 340 ×180 mm. These units are installed aft of the multibeam. The Topas PS40 produces low frequency (secondary) acoustic pulses by non-linear interaction between two high frequency (primary) pulses in the range 35-45 kHz. The secondary low frequency pulses used for sub-bottom profiling are in the range of 1-10 kHz. The system can be operated with both CW and chirp pulses. The source level for a 6 kHz pulse is >204 dB// @ 1m. Penetration occasionally exceeds 50 m in clayey sediments.

4.1.4. Position, heading and attitude

A Kongsberg Seapath 330+ system with the MRU5+ motion and reference unit provides position, heading and attitude data for all mapping systems onboard. This system is dual frequency (L1/L2 band) and derives positions using both GPS and GLONASS satellites. The system handles RTK corrections, which in Swedish waters are received from SWEPOS (<https://swepos.lantmateriet.se/>) through an internet connection. The NTRIP-software used to connect to SWEPOS is the free Open Source Lefebure NTRIP Client (<http://lefebure.com/software/ntripclient/>). Positional accuracy in RTK mode is commonly xy ±2-3 cm and z ±3-6 cm. The potential heading accuracy is according to manufacturer 0.05°. If RTK not is available, the system can make use of the Satellite-based Augmentation System (SBAS) provided by European Geostationary Navigation Overlay Service (EGNOS). The xy accuracy will then drop to be around one meter and the vertical accuracy is commonly around 1.5 m or worse. This implies that if RTK corrections not are available, GPS heights are too imprecise to use for processing the multibeam bathymetry in reference to a given ellipsoid.

4.1.5. Midwater sonar

A Kongsberg EK80 wide-band split-beam sonar is installed in RV *Electra*. Two transducers operating at 70 and 200 kHz respectively, are placed aft of the Topas transmitting and receiving units. The system is capable of producing wideband chirp pulses. The EK80 is operated using Kongsberg's dedicated software, version 1.8.3. The system was last calibrated 26 Aug 2016 near Askö. The acoustic targets used for the calibration procedure are listed in Table 2.

Table 2. Calibration spheres used as acoustic targets.

Frequency	Material	Diameter
70 kHz	Copper	32 mm
200 kHz	Copper	13.7 mm
FM 70/200	Tungsten	38.1 mm

4.1.6. Acoustic Doppler Current Profiler (ADCP)

A Teledyne Acoustic Doppler Current Profiler (ADCP) is installed with a 600 kHz transducer mounted furthest aft of all systems (Fig. 6). The model is Workhorse Mariner, with a max range specified by the manufacturer to 165 m. An ADCP is capable of record current speed and direction underneath the vessel along profiles. The ADCP was not used during the EL17-IGV04 expedition because the focus was on optimizing the high-resolution seafloor mapping and it interferes slightly with the other system and cannot be synchronized.

4.1.7. Water properties (Sound speed, temperature, salinity)

A Seabird 911+ CTD (Conductivity, Temperature, Depth) sampling system is included in RV *Electra*'s standard scientific equipment. This CTD is equipped with 12 Niskin bottles (5 liters). In addition to conductivity, temperature and depth sensors, there are sensors installed to acquire O₂, turbidity, CDOM (Color dissolved inorganic matter), and ChlA (Chlorophyll A) data.

A Valeport MiniSVS is installed in a dedicated pipe running through the hull with its opening end near the multibeam echo-sounder transducers to continuously record sound speed. A Valeport MiniSVP (Sound velocity, pressure) sound velocity profiler is also included in the multibeam equipment to record sound speed profiles at discrete stations.

4.1.8. Acoustic synchronization unit

The EM2040 multibeam, Topas sub-bottom profiler and EK80 split beam midwater sonar can all be synchronized through the installed Kongsberg K-Sync unit. This implies that these three acoustic systems can be operated simultaneously without acoustic interference, which otherwise may result in severely degraded data quality. In particular, the Topas sub-bottom profiler greatly disturbs the EK80 and to some extent also the EM2040. However, running all systems synchronized through K-Sync will not permit that any of the systems use a mode where more than one ping is sent into the water at the time, i.e. so called burst modes cannot be used. The maximum ping-rate will therefore be a standard "round trip".

4.2. Sediment coring and temperature logging

4.2.1. Piston/gravity corer and coring winch

The Stockholm University coring system used on RV *Electra* is based on the large diameter corer designed for Swedish icebreaker *Oden* (Figs. 8-11). The corer is designed using standard metric dimensions of barrel, screws and couplings. It can easily be switched between piston and gravity core mode. The core head measures 859 mm in length, which is 500 mm shorter than the *Oden* core head to fit the handling system on RV *Electra* (Fig. 8). Apart from this, the *Oden* and *Electra* piston/gravity corers are identical. Lead weights of either 68 or 45 kg are used on the core head. During cruise EL17-IGV04 the core head was loaded with 473 kg (Fig. 8). The maximum weight this core head can be loaded with is 563 kg. PVC liners with lengths of 6 m and outer/inner diameter of 110/98.5 mm are used. The trigger weight consists of a 1 m long smaller diameter gravity corer that uses transparent polycarbonate liners with outer/inner diameter of 88/80 mm. The standard piston core release arm is designed so that the lead weights on the trigger weight should amount to 1/10 of the lead weights on the main core head. Figures 8-9 show the rigging, deployment and cutting of liners in 1.5 m sections during the EL17-IGV04 expedition with RV *Electra*. In order to carry out the coring from the aft deck of RV *Electra*, the corer cannot be used with a longer barrel than 6 m. Since the barrels are 3 m in length, a maximum of two barrels can be used. A specifically designed refrigerator is placed on the aft deck for storage of retrieved sediments in 1.5 m long liners sections (Fig. 8). The naming convention of retrieved cores is shown in Figure 11.

The corer is handled using an InterOcean hydraulic winch, model 10031-20HLW, equipped with 600 m of 11.43 mm diameter coax real time data cable (Rochester A302799) (Fig. 8c). Max working load of the cable is 1818 kg and the cable break strength is 7273 kg. The cable is equipped with a SubConn connector permitting the CTD unit to be deployed from the aft deck.

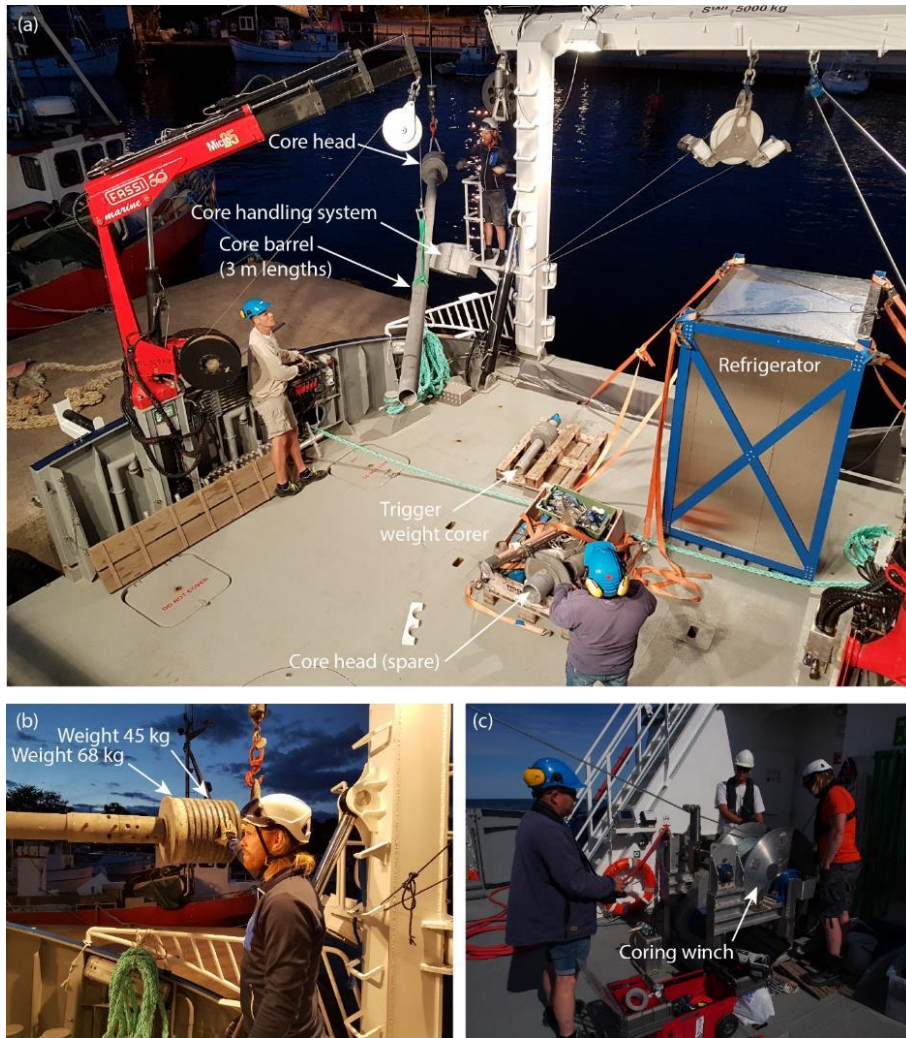


Figure 8. The piston/gravity coring system on RV Electra. (a) Placement of the corer in the handling system is preferably done while at the dock since it involves lifting of the assembled corer with the crane. Once the corer is placed in the handling system it can be fitted with liners, deployed and recovered from the starboard side of RV Electra (Figs. 8-9). (b) Core head with weights. (c) InterOcean coring winch (model 10031-20HLW hydraulic) equipped with 600 m of 11.43 mm diameter coax real time data cable (Rochester A302799).

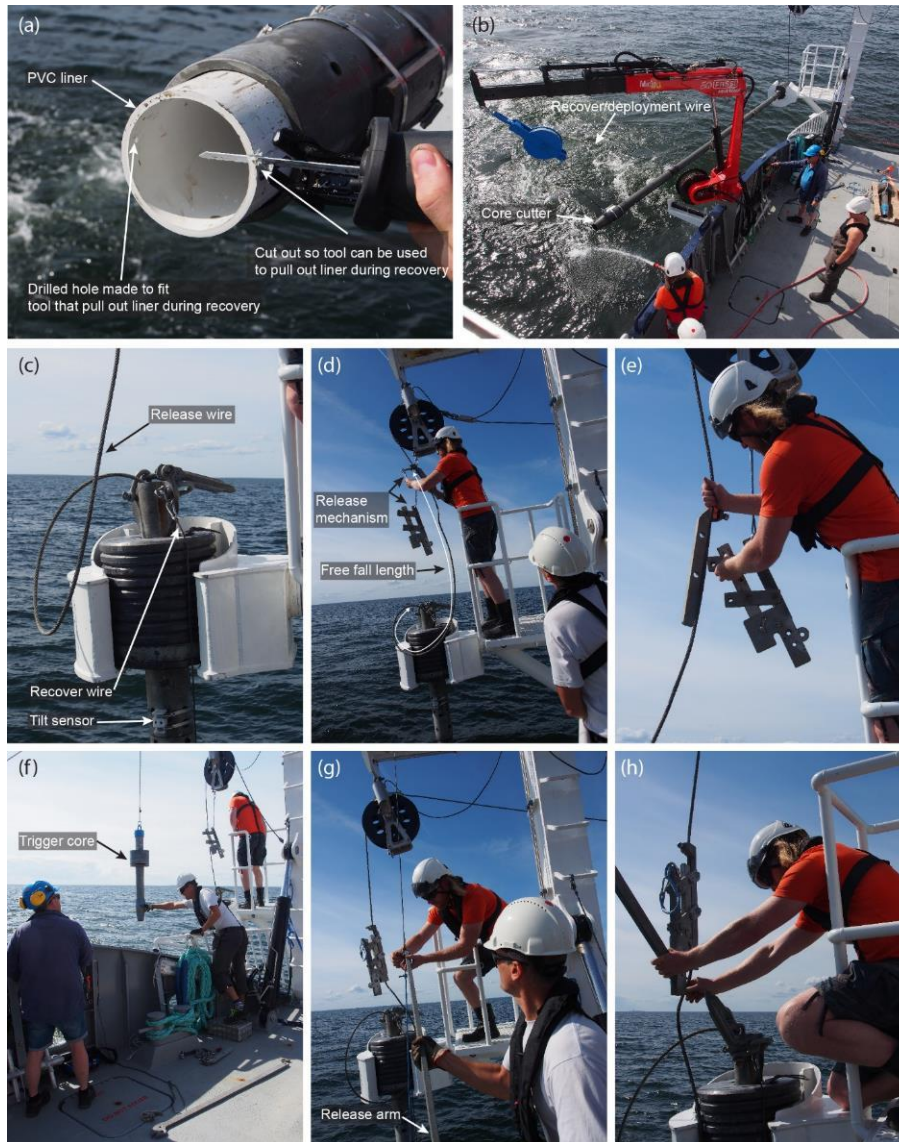


Figure 9. Photos showing the piston coring operation on RV Electra. (a) Preparation of liner in order to make it easy to pull the first bit out after the core cutter has been removed and the liner is filled with sediment. (b) Deployment using the small crane and the deployment/recovery wire, which is attached at the core head during coring. (c) Core head in the core handling unit that pivots. (d-h) Mounting of release mechanism and deployment of the trigger weight corer using the small crane on the starboard side.

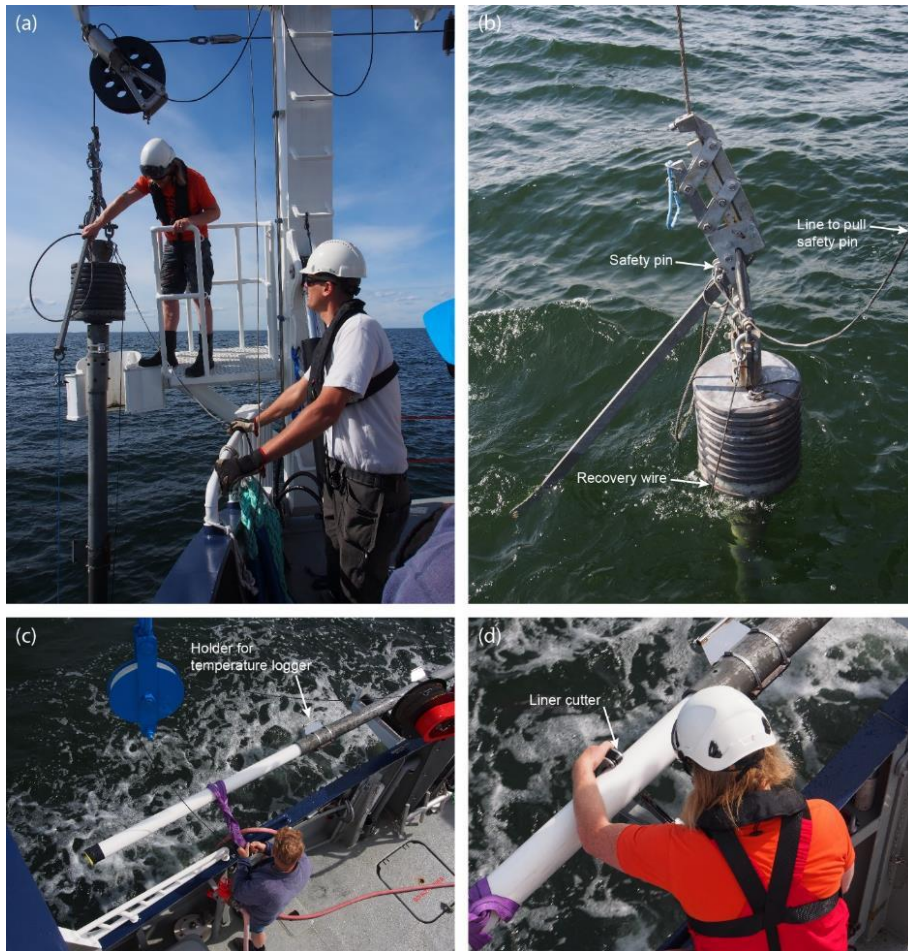


Figure 10. Deployment and recovery of piston corer. **(a)** The corer fully rigged being lifted out of its holder to be lowered towards the seafloor for coring. **(b)** Close-up on the core head and release arm in armed position. Note the recovery wire, which is used once the corer is to be hoisted up to vertical position for the recovery of sediment. **(c-d)** Recovery and cutting of liners into 1.5 m sections. The band coupled to the wire is used to secure the liner section that is being cut since all work is taking place outside of the bulwarks.

EL17-IGV04-01-PC1

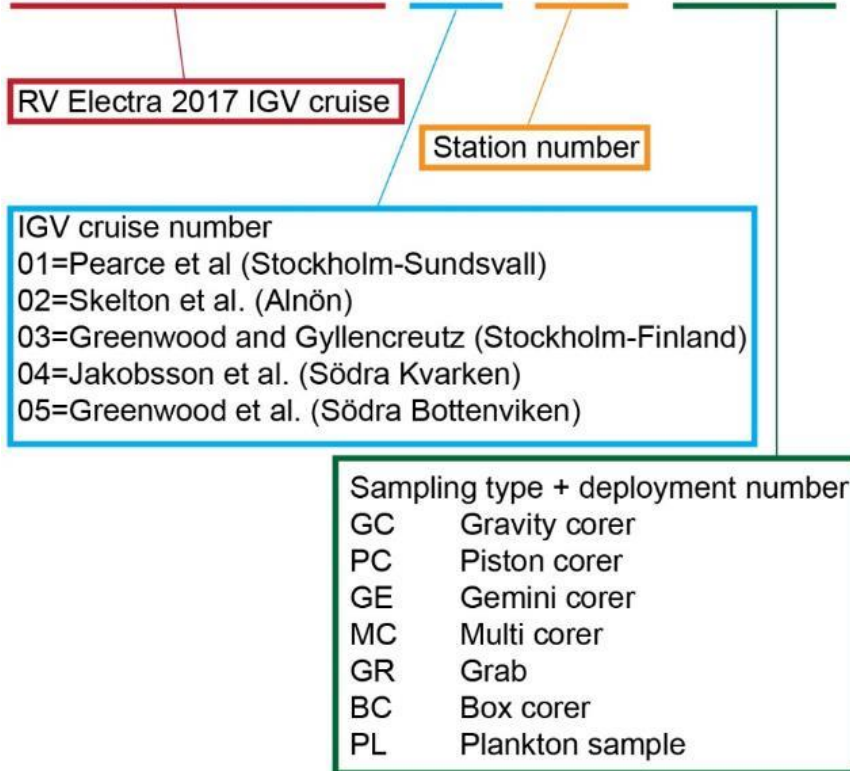


Figure 11. Naming convention used RV Electra cruises with lead PIs from the Department of Geological Sciences (IGV).

4.2.2. Temperature logging

Piston and gravity cores were rigged with miniature temperature probes (16 cm in length by 1.5 cm diameter) manufactured by ANTARES (Pfender and Villinger, 2002) (Fig. 12). The temperature probes allow the in situ temperature to be measured, and in some instances the local geothermal gradient to be determined. The temperature probes were attached to the outside of the core barrel using fins constructed at Stockholm University (Fig. 12). A tilt sensor (DST magnetic), manufactured by Star-Oddi was attached to the top of the core barrel to monitor penetration angles of the cores. The tilt sensors was programmed with a 1s sampling rate, and recorded the ambient temperature, pressure/depth, compass heading, the xyz components of tilt, and ambient magnetic inclination and field strength.

Unfortunately, for each deployment, only 3 temperature probes were attached along the length of the core, with a distance of between 1.5 - 3 m between each sensor. Ideally, more sensors should be used to obtain more detailed information on subsurface variations in temperature, however only 3 of the 15 available sensors were working. The others are now being repaired. Temperature measurements were recorded on a 1s sampling interval and have a resolution of 0.001°C. After penetration, the corer remained within the

sediment for approximately 5 minutes in order to allow for thermal equilibration within the sediments (i.e. for the frictional heat generated during penetration to dissipate). Data was downloaded from each of the sensors between coring casts and initially processed on board to combine the DST-magnetic tilt sensor data with the temperature recordings from each sensor into a single Excel workbook.

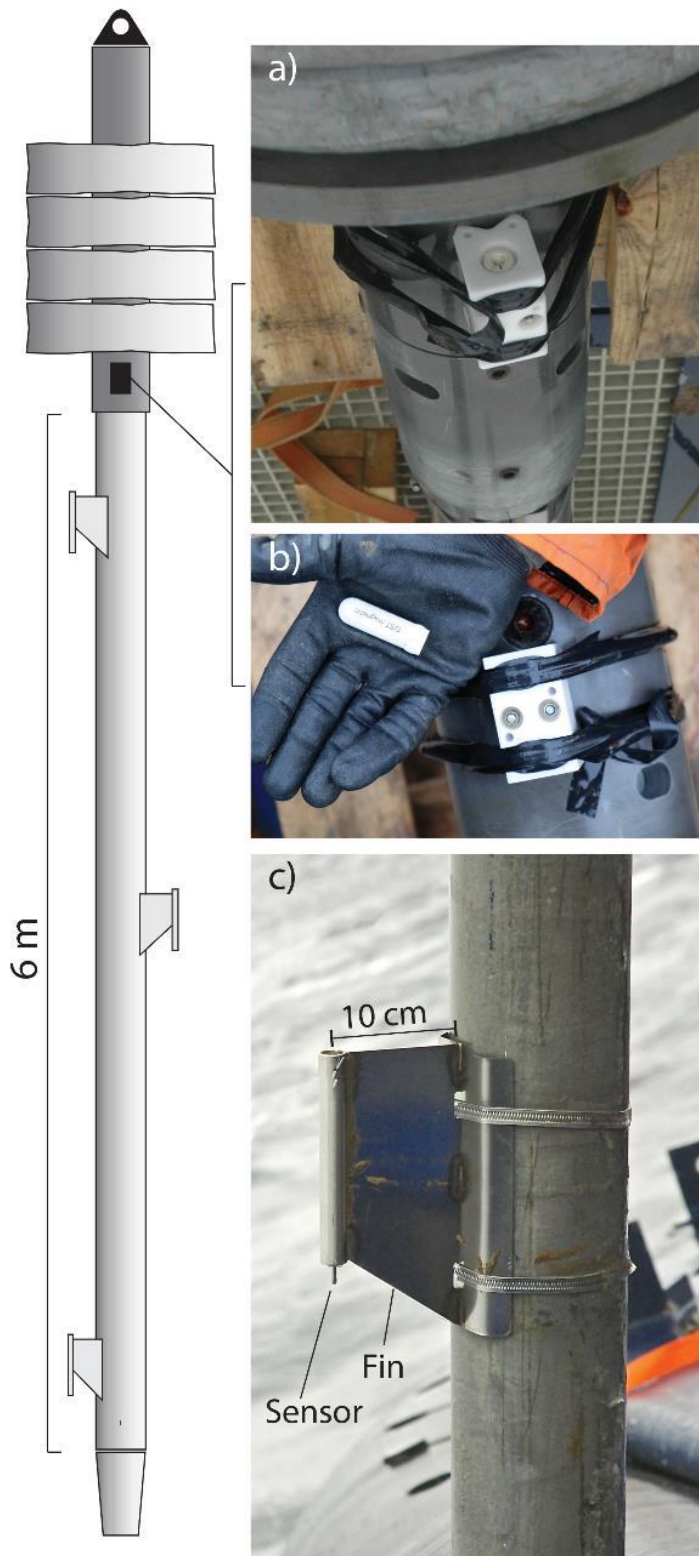


Figure 12. Illustration from O'Regan et al. (2016) showing the sensor attachment to the core barrel of the Stockholm University corer used on IB Oden. The exact same setup was used on RV Electra. The DST magnetic orientation sensor (a, b) was placed at the top of the core barrel beneath the weights. ANTARES temperature probes were mounted in stainless steel fins (c).

4.2.3. Core Logging and Description

Approximately 1 month after the cruise, sediment cores were logged on a Geotek Multi-sensor core logger (MSCL) at Stockholm University. Sensors were oriented in the horizontal direction for whole-core logging. Measurements of the gamma ray derived bulk density, compressional wave velocity (p-wave) and magnetic susceptibility were acquired at a down core resolution of 2 cm. Gamma-ray attenuation was measured using a ^{137}Cs source with a 5 mm collimator and a 10 s count time. Calibration of the system was done each day before logging began, using a machined piece of aluminum that was fit within a section of core liner. The aluminum calibration piece has 4 different thicknesses of aluminum with diameters of 2, 3, 4, and 4.45 cm.

The liner was filled with distilled water and left to equilibrate with room temperature ($\approx 20^\circ\text{C}$). The calibration piece and liner were then placed in front of the ^{137}Cs source. The number of gamma rays passing through each section over a course of 30 s, as well as through an interval containing only water, was logged. The relationship between the measured counts per s [$\ln(\text{cps})$] and the known bulk density of the aluminum/water mixture at each step was determined using a linear fit.

Compressional (p-wave) velocity measurements were made on the MSCL by a pair of automated spring loaded rolling transducers. The travel time of the p-wave between the send and receive transducer is logged. Conversion of the travel time into a p-wave velocity requires calibration to account for delays introduced by the electronic circuitry and those associated with the passage of the p-wave through the liner.

Calibration was performed by measuring the travel time through a water-filled core liner at a known temperature. The temperature and thickness of the water is used to calculate a theoretical travel time (TT) through the water inside the core liner. The difference between the logged total travel time (TOT) and theoretical travel time (TT) is the offset time (PTO). A digital oscilloscope was run during all core logging to monitor the strength of the p-wave signal and to ensure that it arrived within the defined gate interval.

Magnetic susceptibility was acquired with a 125 mm Bartington loop sensor using a 1 s acquisition time. This provided a spatially integrated susceptibility signal that encompasses the entire diameter of the core, with an effective sensor length of generally 4-6 cm. No mass or volume corrections were made to the Magnetic susceptibility measurements.

During logging, small variations in core thickness were also measured and logged using the displacement transducers attached to the p-wave housings. Variations in core thickness, usually more pronounced at the taped and capped core ends, were automatically incorporated into the processed calibrated measurements of p-wave velocity and bulk density.

In the spring of 2021, a Master's student at IGV began a thesis that will integrate the coring, multi-beam and sub-bottom data to describe the marine geology and Holocene paleoceanography of Södra Kvarnen. The 6 sediment cores collected on EL20-IGV04 were split, visually described and imaged.

Descriptions focused on textural, structural and color changes that were used to identify 3 major lithologic units. Additional data on the organic carbon content, grain size and ages of the lithologic units are being generated as a part of the thesis work through 2021-2022.

4.2.4. Bottom filming

A GoPro Hero 4+ camera was mounted on the CTD carousel frame along with light to film the seafloor at the CTD stations (Fig. 13). The GoPro was placed in an underwater housing made by the US Company Group B (model ScoutPro H3) capable of protecting the camera down to 2750 m water depth. The light and its underwater housing were also manufactured by Group B; model Nautilus underwater video light and GPH-1250 general purpose underwater housing. The housing for the light sustains a water depth of 1250 m.

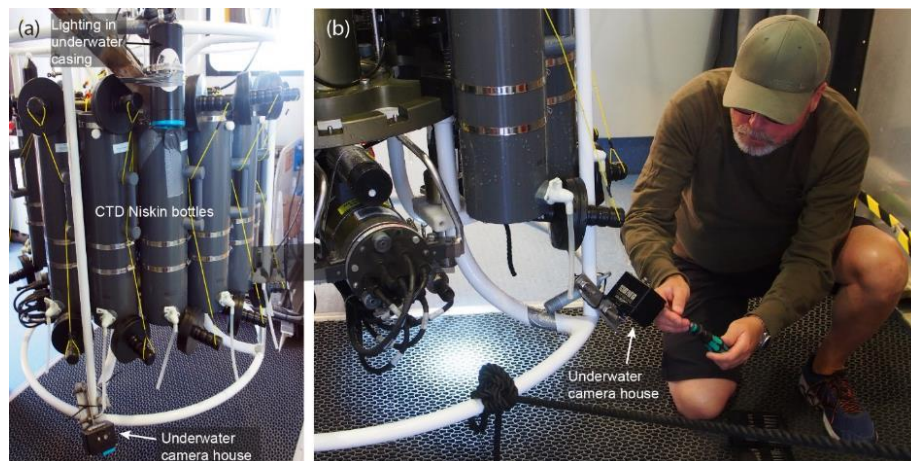


Figure 13. (a, b) A GoPro Hero 4+ was mounted on the frame of CTD carousel in an underwater house capable of sustaining a depth of 2750 m along with underwater light. The underwater casing for the light handles a maximum water depth of 1250 m.

5. Methods - geophysical mapping in Swedish Lapland

In this project we have investigated four Swedish glaciers on their present thermal regime, bed topography and dynamic response to climate signals and we are now in the process of model the way the glacier advances its extent. The methods we have used is mapping the thermal structure of the ice, Structure-from-motion photogrammetry on drone and oblique high resolution photos and numerical modelling.

5.1.1. Radar soundings

A continuous-wave stepped-frequency (CWSF) was operated from a helicopter platform and positions were sampled by a GPS receiver. The radar soundings at Mårmaglaciären were performed in April 7 2017 when snow

conditions are still cold but days are bright and long. The three other glaciers were mapped during earlier field campaigns. The radar system is based on a Hewlett Packard Network Analyzer (8753 ET) (Hamran and Aarholt, 1993, Hamran et al. 1995) and log-periodic antenna. The system gives full control of the transmitted bandwidth, but in this system we are using a center frequency of 820 MHz and a bandwidth of 100 MHz. The radar acquired ~2 records per second giving a trace distance of ~10 m. The collected data was transformed to the time-domain using inverse Fourier transform but no further filtering was done. This radar system has been successful in imaging the thermal regime of polythermal glaciers (Holmlund et al. 1989, Björnsson et al, 1996, Pettersson et al. 2003) and the mapped boundary between the cold surface layer and temperate ice is within a accuracy of ± 1 m (Pettersson et al., 2003).



Figure 14. The radar system mounted on the helicopter on April 7, 2017. Photo Per Holmlund.

5.1.2. Photography and photogrammetry

In later years, photogrammetry has developed quickly as a response to the use of satellite imagery and the use of drones. Drones offer a possibility to make detailed mappings of frontal areas of glaciers and in combination with aerial photography they also provide possibilities to survey geometry changes of the entire glacier. By comparing recent imagery with old volume changes over time has been calculated with a high rate of accuracy. This, in combination with new software for analyses and new mapping tools is a significant development in glacier research.

The method used is named Structure-from-motion and makes use of photogrammetric data from drones and oblique terrestrial and aerial photos making time series of glacier and environmental changes (Midgley and Tonkin 2017). Photogrammetric reconstructions of the shapes of glaciers more than a hundred years ago is a vital tool for understanding glacier dynamics.

And the fact that no glacier surges has been observed and documented in Scandinavia does not necessarily mean that surges have not occurred in the past. Thus, surgelike glacial advance can be an important process for landscape formation in Scandinavia. Further, surges may have been important during cold climate events in Scandinavia. For example, during the Little Ice Age temperatures in the Swedish mountains were well as low as they are on Svalbard today (Alexandersson and Eriksson 1987, Holmlund 2020) and surges could have been usual.

In this study we have used an ordinary standard professional camera (Nikon 800D). It serves the mission well with a 36 mega pixel sensor. This hand held camera was used for re-photography from ground points (used in the past as photo points) and mapping by oblique photography from a helicopter. The orthophoto produced has a resolution of about 0.5 m. We have also used a drone (DJI Phantom 4) which has shown the usefulness of such equipment. It takes about 1,5 h and about 1000 vertical photos to map a one square kilometer frontal area in detail. The resolution is about 10 cm.



Figure 15. Drone mapping in front of Rabots glacier on August 4, 2018. Photo Per Holmlund



Figure 16. Aerial photography from helicopter with open door. August 5, 2018. Photo Per Holmlund

5.1.3. Data processing

When drones are used in field, a digital flight plan is made manually in advance, using any previous elevation data. With a digital flight plan, the drone carries out the mapping automatically. This can easily be executed using the commercial software UGCS Pro. It is possible to map without a digital flight plan, facilitating unplanned missions, but is less redundant and requires thorough manual input.

The post processing of collected data can be summarized in the steps below:

- A. Calculating the distortion parameters of the camera used. This involves photographing calibration patterns on a screen, but is often done automatically to a sufficient degree of accuracy in the subsequent step below.
- B. Aligning the images to each other, and refining calibration parameters. This is a predominantly automatic process, but sometimes needs manual input, by defining recurring points between the images (big rocks, snow patches etc.).
- C. Defining previously collected ground control points (using GPS, or other produced models), for georeferencing the model.
- D. Creating a point cloud, consisting of millions of triangulated points, that were identified in two or more images. This is a completely automatic process, resulting in a Digital Terrain Model (DTM).
- E. Producing orthophotos, by draping the geometrically corrected images on the produced DTM.

The workflow A to D is often iterative, as step D is where qualitative and quantitative accuracy evaluation is first made possible. If the point cloud

shows clear errors, the faulty areas can be improved upon in subsequent iterations of the process. The software of choice for data processing is Agisoft PhotoScan Professional Edition. Data on ice dynamics is basically taken from our own high frequent radar data on the thermal structure of glaciers in Sweden (Holmlund et al 2016). A paper on size changes of the summit of Kebnekaise was produced within this project describing the methodology (Holmlund and Holmlund 2018).

6. Results - marine mapping and coring

6.1. Geophysical mapping from RV Electra

An area of 70 km² was multibeam mapped inside the survey box and 84 km sub-bottom profiles and 58 km midwater profiles were acquired (Fig. 17). The individual sonar systems were not run simultaneously using K-Sync because each acoustic mapping system was optimized to acquire the highest resolution possible. For example, the Topas PS40 sub-bottom profiler was operated using “burst mode” permitting multiple pings in the water rather than in “normal mode” when each return echo is recorded before transmitting the next ping. K-Sync requires normal mode to operate. In addition, sub-bottom and midwater profiles were acquired in a regular grid pattern in order to facilitate the geological/oceanographic interpretation. The main purpose of the geophysical mapping was to search the area for any signs of mass wasting and and/or tectonic movements following the retreat of the SIS. Evidence for current activity in the survey area quickly became obvious in the acquired geophysical mapping data. For this reason, a large part of the survey was dedicated to map details permitting current induced seafloor features to be distinguished from features related to mass wasting or tectonic activities.

Detailed compiled bathymetric information of the seafloor inside Swedish territorial waters is subjected to restrictions under Swedish law (Säkerhetsskyddslagen, 1996:627). The geophysical mapping data published in this report have been granted to be released for public view and access by the Swedish Maritime Administration (permit 17-03187).

6.1.1. Multibeam bathymetry

The geophysical mapping program was initiated with multibeam echo sounding after CTD station CTD01 was completed in the southernmost part of the survey area in order to provide the multibeam system with an up-to-date sound speed profile (Fig. 117). Mapping was generally carried out with a 300 kHz pulse and with 100 % overlapping swaths between survey lines (Fig. 18). The 400 kHz inspection mode was only used briefly when passing the wreck August Thyssen (Fig. 19). The ship speed was kept between 5 and 6 knots in order to get enough along track resolution.

The huge depth variation in the area comprised a great challenge due to the resulting large variation in swath coverage (Fig. 18). Survey lines could not

be kept straight in order to keep a swath overlap of 100 %. This was also one of the reasons for that the sub-bottom and midwater profiles were acquired separately. The multibeam bathymetry was only initially post-processed during the expedition using the CUBE algorithm in the Qimera software. Further post-processing will include manual cleaning and inspection as well as referencing the depths to the SWEN2008_RH2000 geoid model using the ellipsoidal height information from the RTK GPS. The water level varied during the two survey periods between 12 and 22 cm above the RH2000 reference level at SMHI's station 2170 located in Forsmark (Fig. 20).

The average depth (uncorrected for variations in water level) of the multibeam mapped area is ~155 m. The shallowest recorded depth of 2.7 m (uncorrected) was recorded where RV *Electra* ran aground east of Understen island, while the deepest depth of nearly 254 m was logged in the southeast corner of the mapped area.

The seafloor is heavily marked by bottom currents sweeping along the steep scarps (Figs. 21 and 22). Along the current eroded channels are large sediment accumulations, likely comprised of the eroded sediment. The abundant signs of strong bottom current activity is not surprising considering that Södra Kvarnen comprises the main deep connection between the Baltic Sea and Gulf of Bothnia. In addition to seafloor traces of current activity, the multibeam reveal signs of mass wasting and buried channels. The wall of the eastern ridge has at one place collapsed over a large area (Figs. 21 and 22). Mass wasted material is located below the collapsed wall. North of the two prominent ridges, a channel system appears to be buried underneath a drape of sediments (Fig. 22).

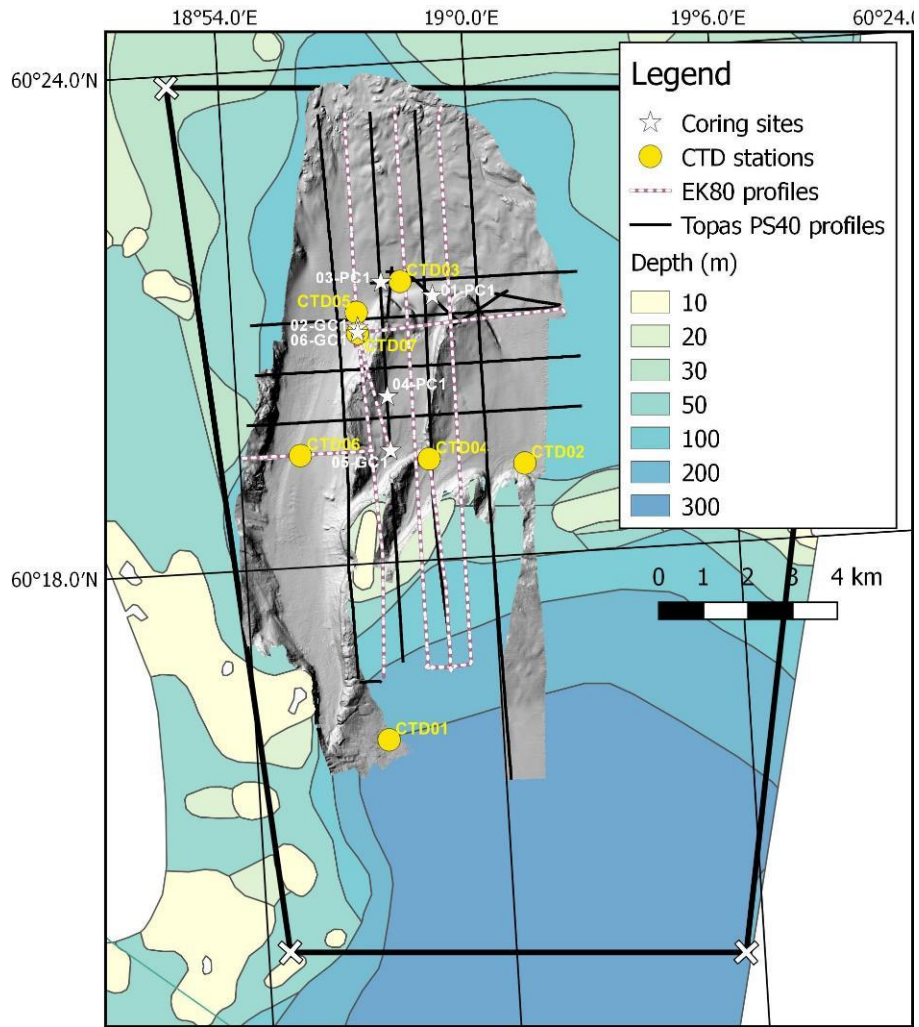


Figure 17. Acquired geophysical mapping data, sediment cores and CTD stations during expedition EL17-IGV04. The background bathymetry is from the Geodataportal (<https://www.geodata.se>). The thick black polygon outlines the survey area in focus.

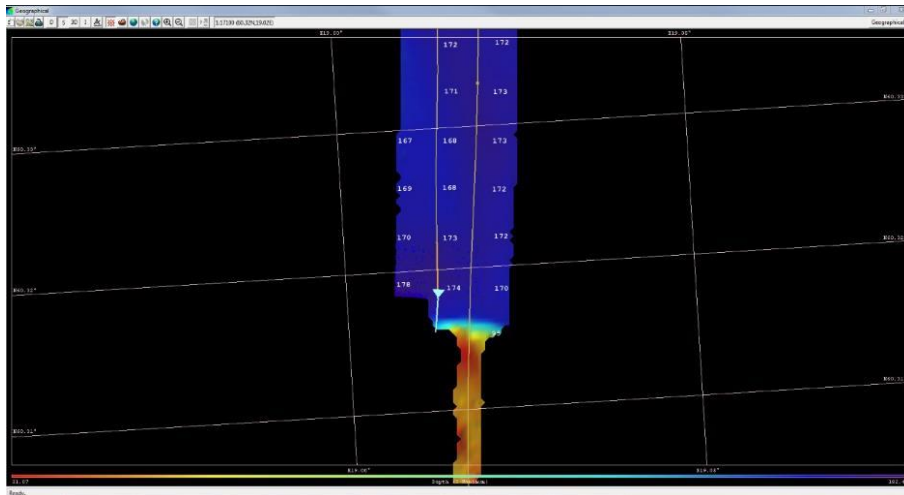


Figure 18. Screen dump showing data collection during expedition EL17-IGV04 using Kongsberg's multibeam acquisition software SIS. The image shows how the survey was carried out with 100 % overlapping swaths. In addition, the problem caused by large depth variations with respect to keeping 100 % overlapping swaths is clearly seen by the narrow swath width in the shallow south end of the area covered by the screen dump.



Figure 19. Multibeam image of ship wreck of August Thyssen at 58 m water depth. The 90 m long ship sunk in 1940 after hitting a mine. She was transporting Swedish iron ore.

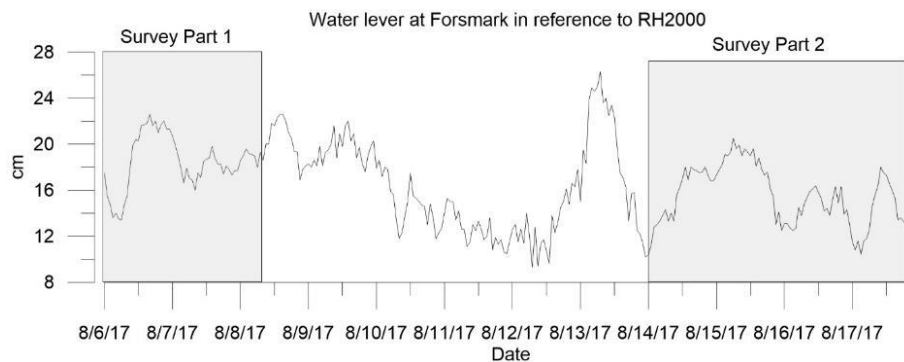


Figure 20. Water level at SMHI station 2170 located in Forsmark. The grey boxes shows the two survey periods.

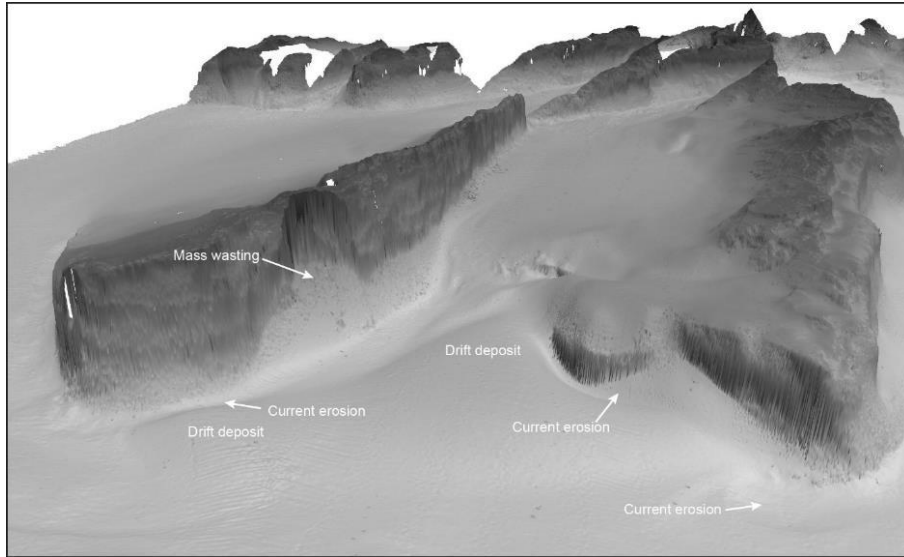


Figure 21. 3D visualization of the multibeam bathymetry revealing strong bottom current activities and mass wasting. The view is from north to south.

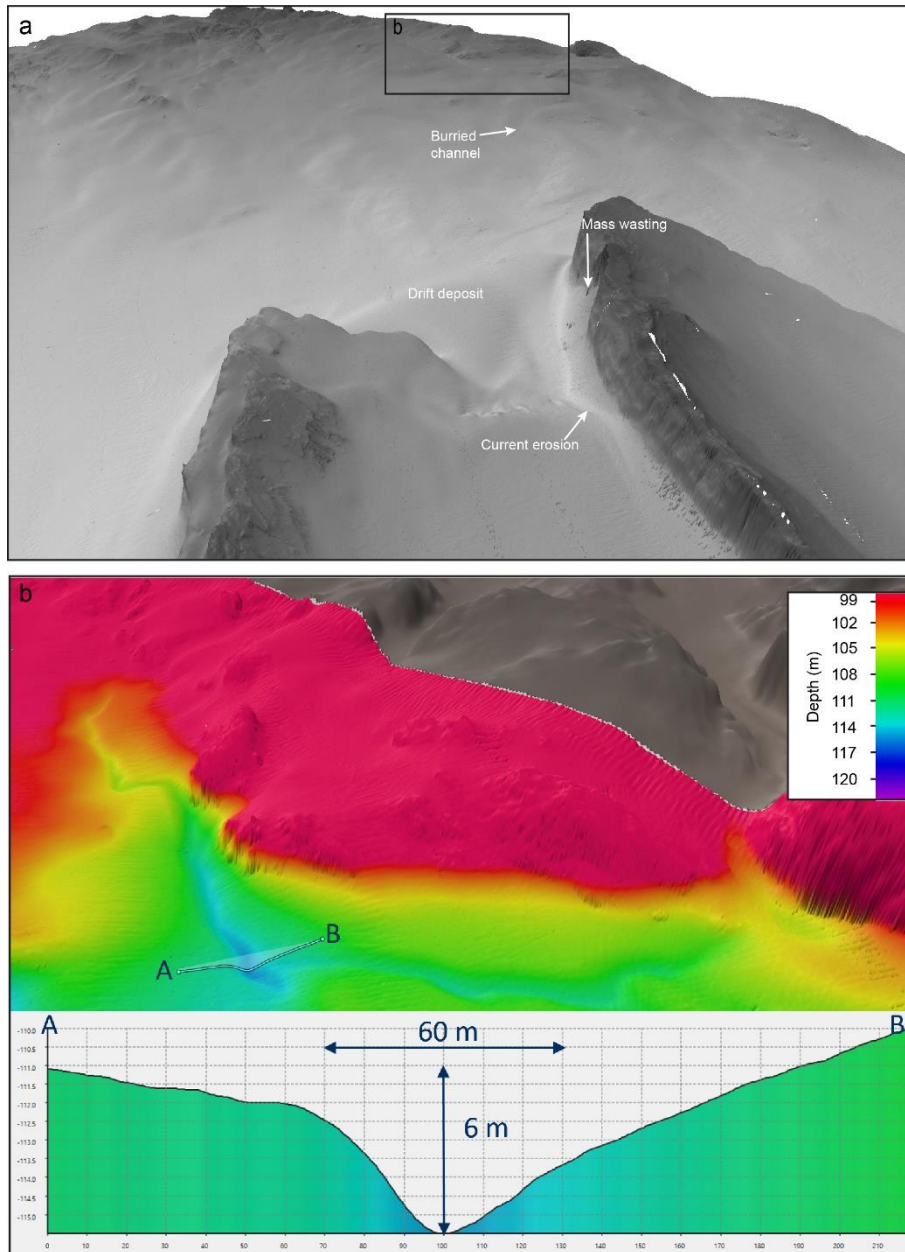


Figure 22. a) 3D visualization of the multibeam bathymetry looking north from the two prominent ridges. **b)** Zoom in on area where sharp channels are discovered in the seafloor topography. The sharp nature of these together with their spatial appearance suggest that they may not be regular erosional channels from bottom current induced gravity flows, they could instead have been initiated by movements in the crust below. Further analyses are required.

6.1.2. Midwater

The Simrad EK80 files (.RAW format) were parsed and further processed with scripts run in MATLAB version 2016a. All data were corrected for spherical spreading and acoustic absorption. Acoustic absorption profiles were calculated using temperature, salinity, and pressure data from CTDs taken during survey operations and applied using a nearest in time regime. Resulting

data are plotted in all figures as sound pressure levels (dB) at a range (m) from the transducer face.

Transects of the survey area were run in conjunction with the sub-bottom profiling lines, both parallel to multibeam survey lines (north-south) and perpendicular (east-west) (Fig. 17). Figure 23 shows the location of the EK80 east-west transect line in the southwest corner of the survey area shown in Figure 24; data from both the ES70 (50-90 kHz) and ES200 (160-250 kHz) transducers are plotted.

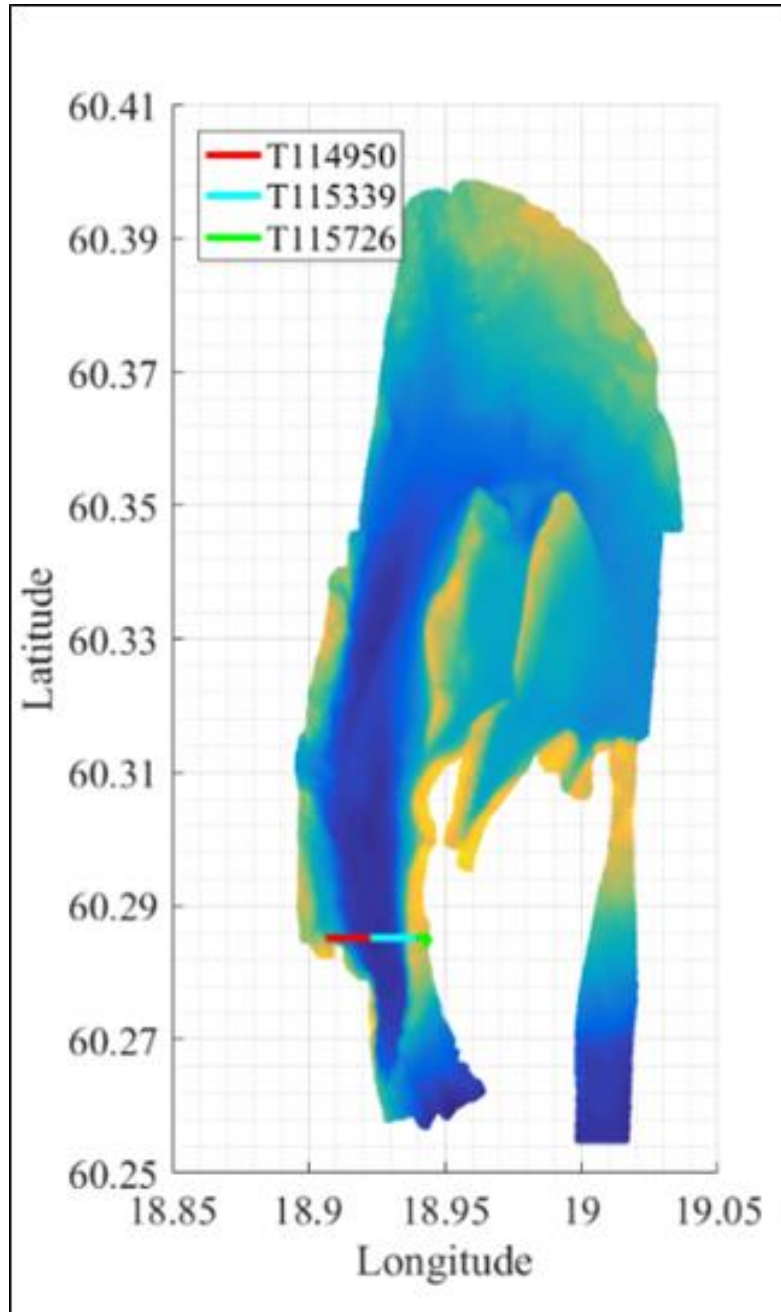


Figure 23. Location of east-west EK80 line shown in Figure 20. Line colors correspond to individual EK80 lines.

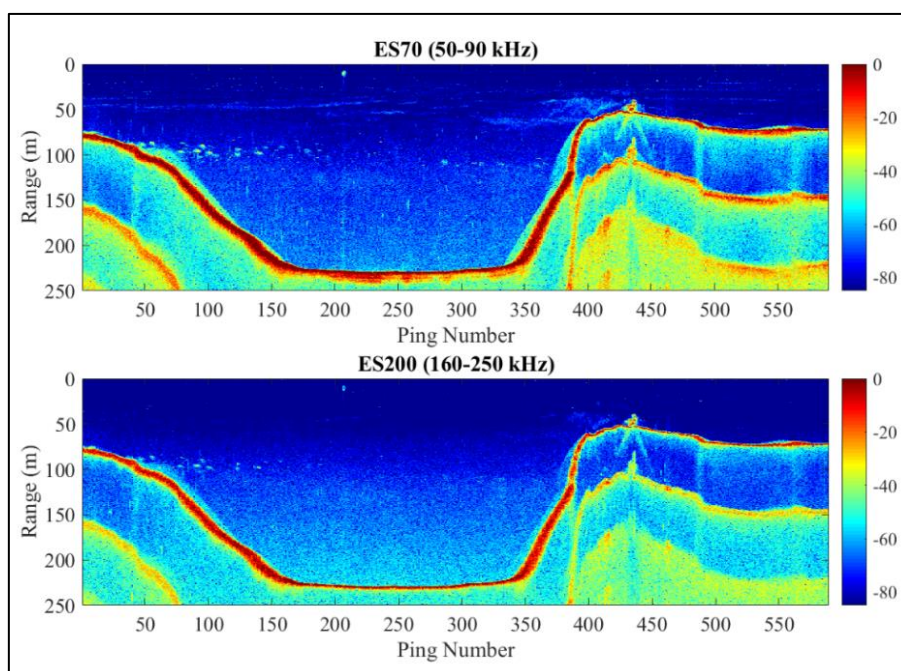


Figure 24. EK80 water column sound pressure data plotted as range from transducer face (in meters) for successive pings. Transect is a concatenation of the three files shown in Figure 19.

Water column features such as fish and horizontal layer structures can be identified in the both the ES70 and ES200 echograms. The ES70 record has less noise, especially at depths >100 meters, resulting from higher power (300 W) and lower frequency pulse. Some subsurface structure can be seen in the ES70 record.

In the upper 75 meters of the water column there are many horizontal, layer-like acoustic anomalies throughout the echogram (Fig. 24). These layers are the product of density changes in the water column from thermohaline structure or biological scattering from phytoplankton conglomerations. The impedance contrast from the change in density at layer interfaces causes acoustic scattering. Throughout the survey area one such acoustic anomaly layer persists at the approximate depth of the thermo- and halocline as determined from CTD casts. Additional layers are likely the result of small scale structures within the water column.

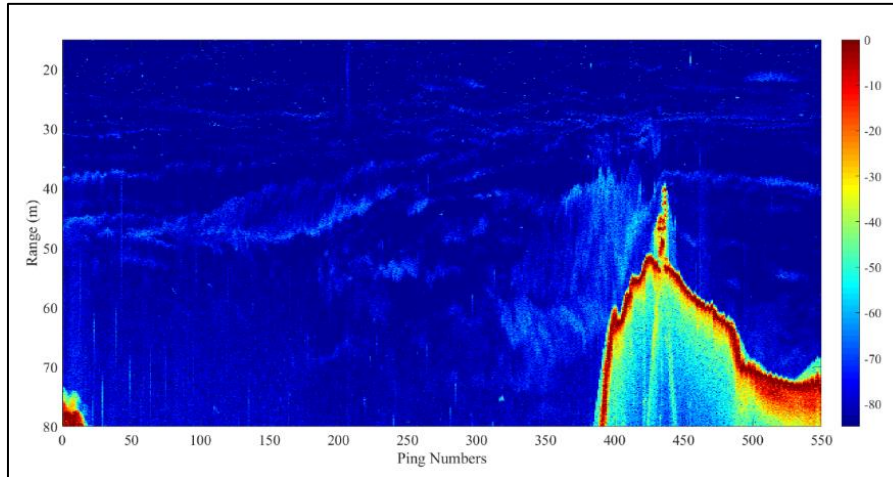


Figure 25. EK80 echogram (45-90 kHz FM pulse) showing apparent horizontal density layer anomalies in upper water column and a cross-section of the ship wreck of August Thyssen identified in the multibeam data (ping 438-448, 38-58 m depth).

The EK80 was run during several CTD cast operations to provide direct physical property data (temperature, salinity, oxygen, etc.) at horizontal density anomaly locations. Figure 26 shows an example of these operations. At a depth of approximately 12 meters the CTD rosette enters the beam of ensonification and the CTD cast path can be traced through many density anomaly layers during descent and ascent.

From CTD data the approximate reflection coefficient (function of sound speed and density of medium) at layer interface can be calculated from the temperature and salinity data. A reflection coefficient can also be derived from the echogram scatter strength if the EK80 data has been calibrated for beam pattern effects and transducer sensitivity.

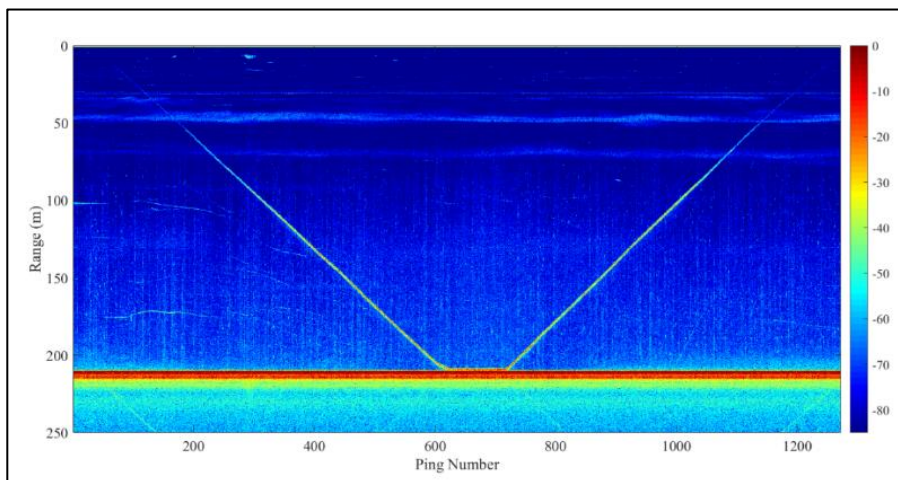


Figure 26. EK80 echogram during CTD cast. CTD rosette path intersects horizontal density layers in the upper 65 meters.

One possible seep feature was identified during August 14th survey operations (subsequent data processing may uncover additional seeps). The seep feature is identified by the vertical grouping of increased sound pressure values (Fig. 27). The seep feature sits at the base of a steep slope feature, at a depth of approximately 200 meters, and disappears at approximately 150 meters depth. No individual bubble scattering can be identified within the seep feature and there is no visible gas blanking in the subsurface associated with the fluid release location.

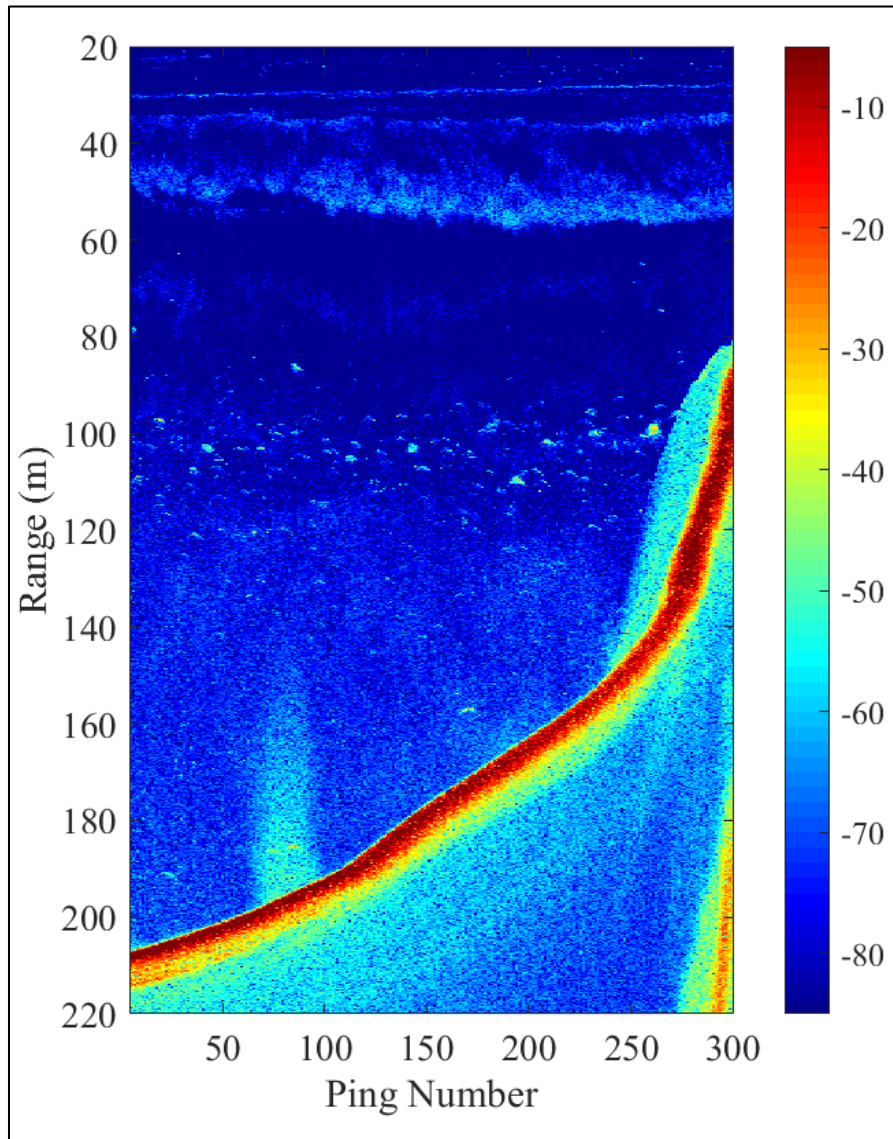


Figure 27. EK80 echogram showing vertical acoustic anomaly starting at seafloor (~200 meters) and rising approximately 50 meters in water column to termination at 150 meters.

6.1.3. Sub-bottom profiling

The sub-bottom profiles provide information about the sub-seafloor sediment stratigraphy, with penetration exceeding 50 m in parts of the surveyed area. The west-east sub-bottom profiles show the dramatic bottom topography (Fig. 28.). The shallowest peaks only have a thin veneer of sediment while the basins in between are filled with > 50 m of sediment in the deepest parts. Mass wasted sediment are clearly identified in the profiles at the base of the steep slopes. Sediment cores EL17-IGV04-03-PC01; EL17-IGV04-04-PC01 and EL17-IGV04-05-GC01 were positioned along sub-bottom profile 20170814074535 (Fig. 29).

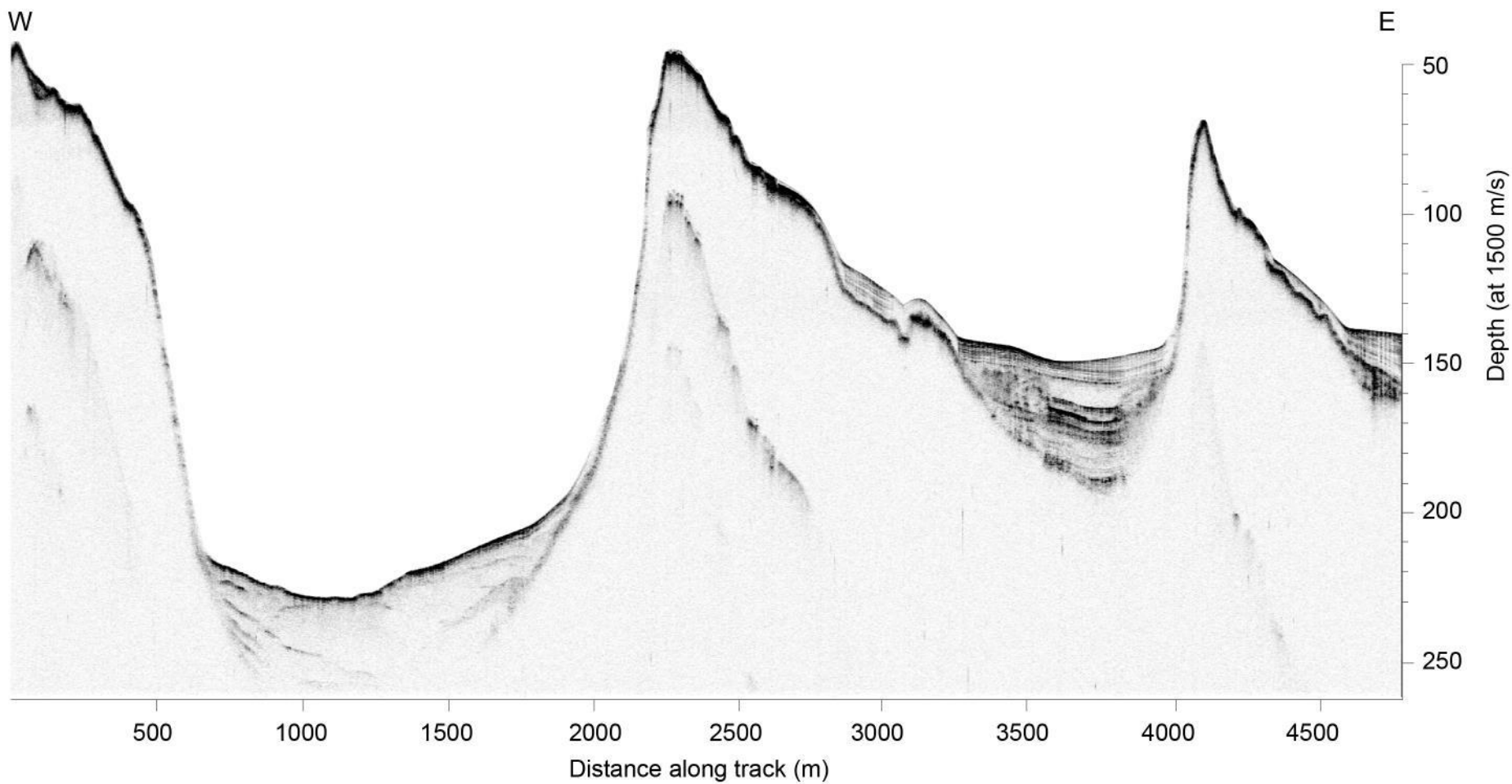


Figure 28. East – West subbottom profile across the bathymetric highs in the survey area.

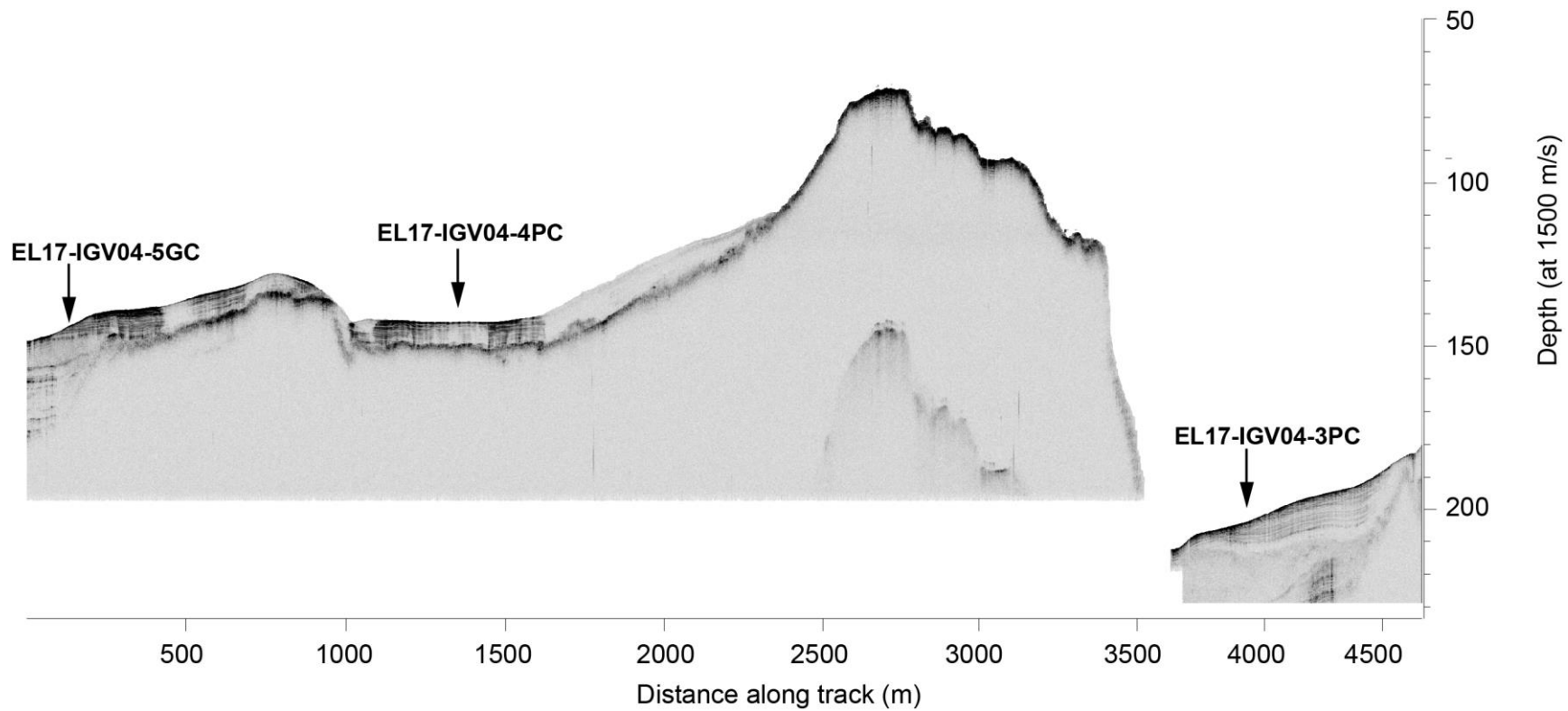


Figure 29. Sub-bottom profiles acquired from south-north along where the sediment cores acquired.

6.2. Sediment coring

Six sediment cores were acquired on the expedition, 3 piston cores and 3 gravity cores, the curated length and coring targets are summarised in Table 3, with complete coring sheets attached in the Appendix Core logs. The locations of the coring stations are presented on Figure 17 with details of the sub-bottom stratigraphy at each site shown in Figure 30.

Table 3. Retrieved cores and the length of acquired sediments. Further information about the cores is included in Appendix Core logs.

Core	Length (m)	Target
EL17-IGV04-01-PC01	4.77	An apparent drift deposit exhibiting possible gas blanking in the subbottom data
EL17-IGV04-02-GC01	4.00	Western slope of westerly rotated fault block where acoustic data suggested gas flares coming from the seabed.
EL17-IGV04-03-PC01	4.29	Older strata underlying a thin veneer of current eroded sediments (Fig. 29).
EL17-IGV04-04-PC01	5.04	Acoustically laminated sediments possibly recording uninterrupted modern and recent sedimentation (Fig. 29).
EL17-IGV04-05-GC01	5.70	Older strata underlying eroded younger sediments penetrated by 04-PC01 (Fig. 29)
EL17-IGV04-06-GC01	5.36	Core positioned where a seep was observed in EK80 data (Fig. 27). Seep not seen when we returned to core.

Cores were split and described after their physical properties were measured using a Multi-Sensor Core Logger (MSCL). The MSCL provided good quality measurements of sediment bulk density (BD) and magnetic susceptibility (Ms), but more limited data on the compressional wave velocity (Fig. 32 and 33). This is not unusual as the P-wave signal is strongly dependent on the core liner being completely full of saturated sediment. Small amounts of air surrounding the sediments inside of the core liner result in a poor acoustic coupling between the transducer and receiver. This results in either a complete loss of the signal, or a severe degradation of its amplitude, which prevents the automatic peak recognition of the software from working accurately.

The visual core descriptions and MSCL data allow an initial interpretation of core lithologies, which will be more fully developed and integrated with the sub-bottom data and attempts to date the sediments in an MSC project being completed at IGV in 2022 by Anton Wagner.

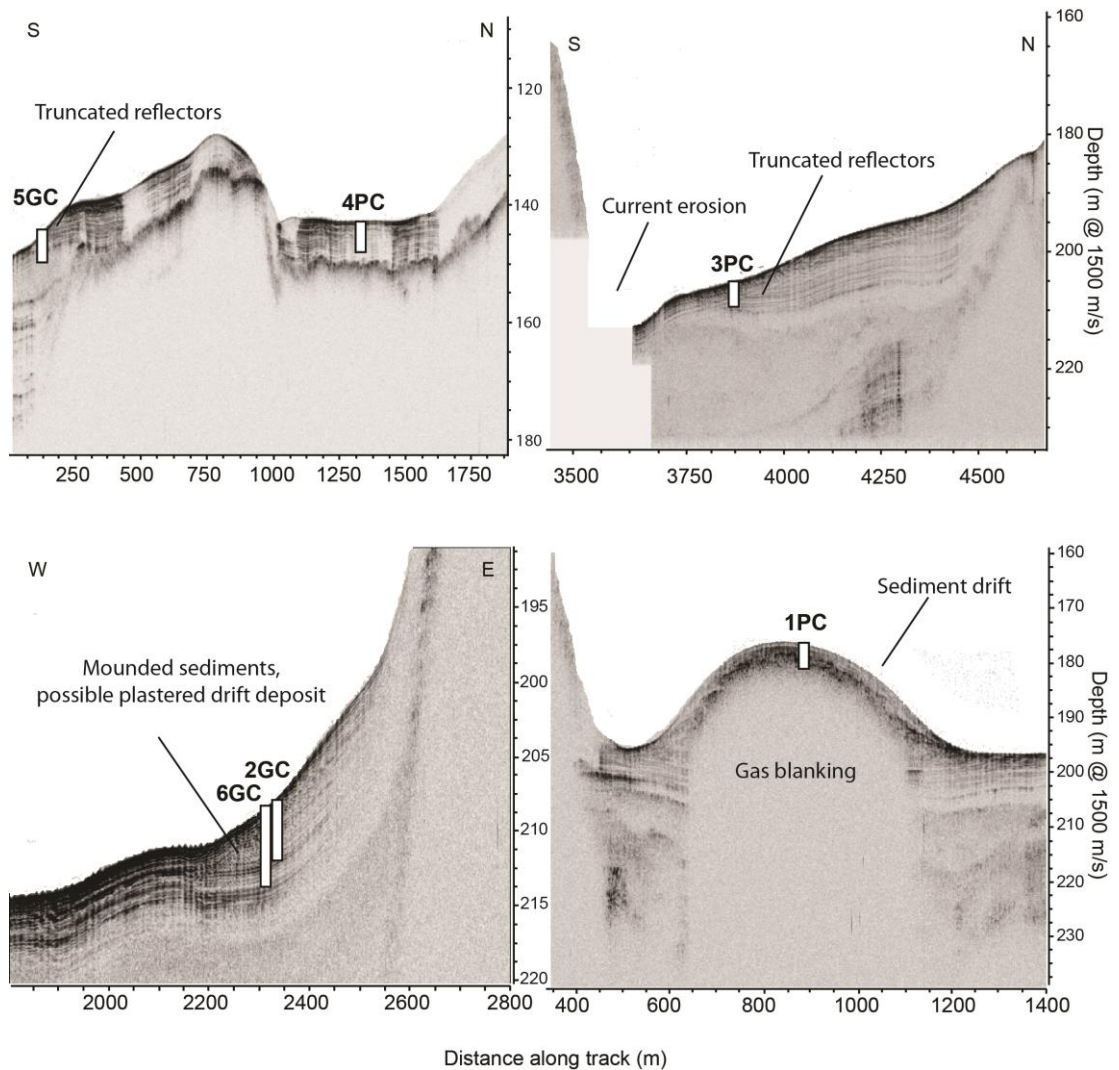


Figure 30. Sub-bottom data illustrating the location, setting and approximate penetration depths of the 6 cores. Core 6- and 2-GC01 are projected onto the closest E-W sub-bottom line.

6.2.1. Core Lithology

Overview

The sediments described in the 6 cores were broadly divided into 3 major lithologic units (LUs). Individual core descriptions and section images are presented in the Appendix Core Logs.

LU1 is found in all the cores except EL17-IGV04-01-PC01. It is identified by texture and grain size, and is a coarse-grained sand to silty sand deposit that ranges in color from black through brownish grey to dark greenish grey (Figure 31 a-b). LU1 is coarsest at the surface and fines downcore with a gradual transition into LU2 within the upper few cm's to dm's below the seafloor. Its prevalence throughout the survey area is consistent with modern bottom-current scouring of the seabed (Figure 21) which is evident in the detailed multibeam mapping.

LU2 is a clayey silt to silty clay that often contains intervals of black sulphide banding/mottling and discrete finely laminated intervals interspersed with more massive intervals. It is identified in all cores and appears to change in color, texture and structurally (by the more pronounced presence of laminations) as the sediments gets older. Generally, it is either black to dark greenish grey in the near surface with abundant but variable black sulphide coloring (Fig. 31c-e) and transitions into a bluish grey clayey silt with more pronounced and abundant laminated intervals (Fig. 31 f-g) in the lowermost parts of EL17-IGV04-02-GC01, 6-GC01, and above potentially unconformable transitions into LU3 in cores 3-PC01 and 5-GC01.

LU3 is a greyish brown silty clay that is massive in 3-PC01 (Fig. 31h), but laminated in 5-GC01 (Fig. 31i-j). In both cores it is capped by a very firm black clay layer. In 5-GC01, the laminations are severely deformed, most pronounced near the top of the unit. LU3 is generally interpreted as older glacial to post-glacial clays that correlate to truncated sub-bottom reflectors that outcrop at or near the seafloor (Fig. 30).

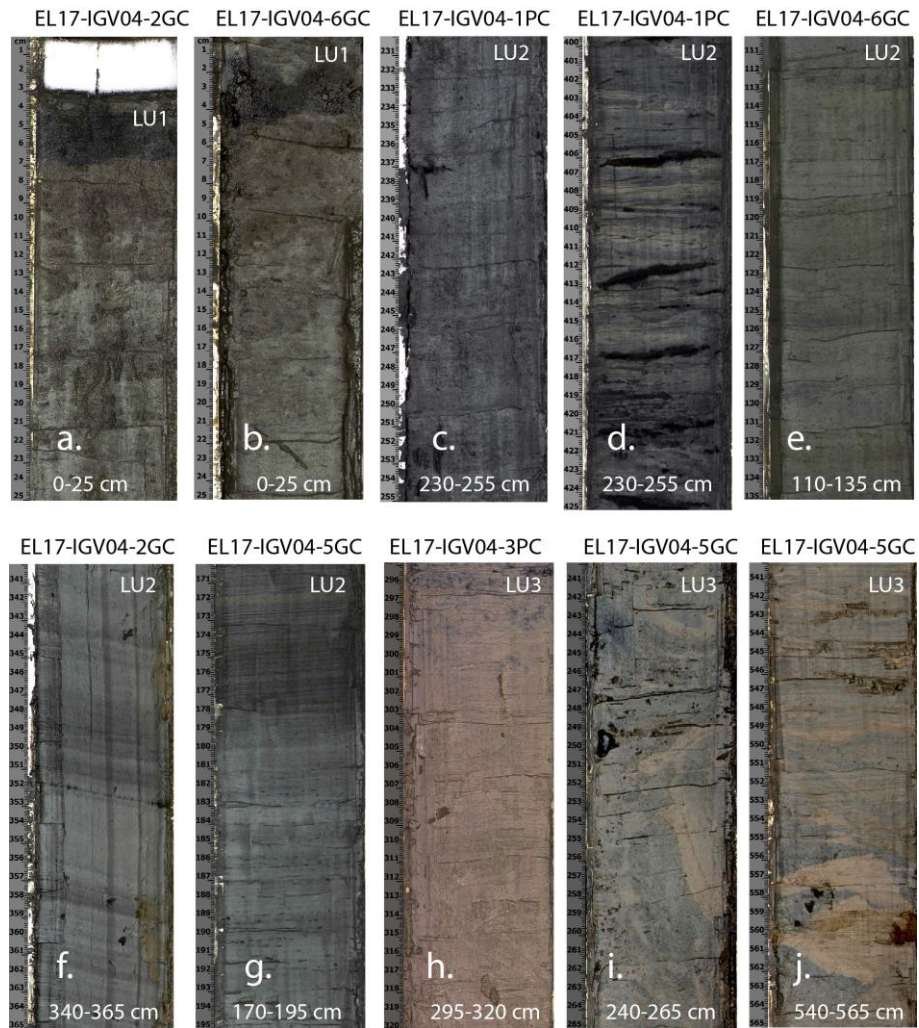


Figure 31. Representative images of the major lithologic units. LU1 (a,b); LU2 (c-g) and LU3 (h-j).

EL17-IGV04-1-PC01

The entire core is assigned to LU2. In the upper 3 sections, the sediments have a very low bulk density ($\sim 1.2 \text{ g/cm}^3$) and low susceptibility ($5\text{-}15 \text{ SI} \times 10^{-5}$) (Figure 32). They are typical of organic rich Holocene sediments from the Baltic. At approximately 3 m core depth there is a notable increase in the bulk density. Below this bulk density drops to values below 1 g/cm^3 . This is physically impossible for saturated marine sediments, and indicates that the sediments were no longer at 100% saturation. This is consistent with the core descriptions that illustrate the lowermost part of this core is fissile and contains numerous large (cm scale) cracks. There is no notable change in magnetic susceptibility across this transition, and the color changes that are seen (patchy occurrence of greyish brown sediments in a dark greenish grey matrix) are consistent with oxidization. Furthermore, grain size does not appear to change across the transition where the bulk density increases, suggesting that the color and density changes may be related to diagenetic processes (Fig. 32). As the core was recovered from a drift-like deposit with pronounced gas blanking beginning a few meters below the seafloor (Fig. 30), the origin of the cracking

is likely from gas escape upon recovery and prior to core logging. It is not yet clear why this sudden transition occurs a few meters below the seafloor.

EL17-IGV04-2-GC01 and 6-GC01

These two cores were collected close to one another (Fig. 30) at the base of one of the steep ridges, where mounded sediments appear to have been deposited under the possible influence of current activity. Sediment core EL17-IGV04-6-GC01 was positioned where a seep was observed in EK80 data. The seep was not seen when we returned to core and there was no evidence of gas escape in the core. These cores have the same lithology with near identical downcore physical properties (Figs. 32 and 33). The major difference is that 6-GC01 penetrates deeper than 2-GC01. Both are capped by a pronounced sand layer that over the course of ~40 cm fines downcore where LU1 gradually transitions into LU2. This is reflected in the MSCL data by the high initial bulk density and magnetic susceptibility, which then decrease towards the base of the unit (Figs 31 and 32). Just below LU1, both cores contain an interval of moderate BD (1.3-1.4 g/cm³) and low Ms (5-15 SI x10⁻⁵) assigned to LU2. A slight increase in both these parameters accompanies the transition into the more greyish-blue and occasionally laminated sequence that appears near the base of LU2 (Figs. 31f-g). In the deeper penetrating 6-GC01, a non-conformable contact with another thick sand layer occurs at around 460 cm core depth (seen in the MSCL data by a peak in Ms and BD). This has the same characteristics as the surface sand layer. It is capped by black sand and underlain by brown sand that fines downwards. The underlying sediments remain in LU2 but appear disturbed and contain numerous smaller < 1 cm thick sand layers. Core 6-GC01 therefore may penetrate the base of the mounded sediments that are found along the base of the steep escarpment. Dating of sediments above and below the lowermost sand layer may establish whether there is a large unconformity present, and constrain the onset for drift deposition.

EL17-IGV04-3-PC01

The core was collected on the edge of a shallow current eroded channel that exists along the headland of the westernmost ridge. Presumably, the northward flowing current also influenced deposition at 2-GC01 and 6-GC01. In sub-bottom data, 3-PC01 was positioned to penetrate a couple meters of draping sediment overlying older, truncated outcropping reflectors (Fig. 30). This core is also capped by a sand layer (LU1) that gradually fines downcore in the upper 11 cm as seen in the core description and reflected in the MSCL data by the uppermost interval of high BD and Ms. This is consistent with a strong modern day bottom current influence on sedimentation. LU1 overlies sediments assigned to LU2, which gradually increases in bulk density and magnetic susceptibility as they transition into the more frequently laminated bluish-grey sediments between 200-300 cm core depth. A peak in magnetic susceptibility at 2.46 mbsf is not accompanied by a change in the bulk density and could not be tied to any visual change in the core lithology. Thus it may indicate the presence of a clast that was not detected by the narrow gamma-ray beam used to measure bulk density. Both the BD (> 1.6 g/cm³) and Ms (> 20 SI x10⁻⁵.) attain peak values in LU3, which is a massive brown consolidated clay. This lithology likely comprises the older outcropping reflectors seen at the site in the sub-bottom data, and appears to be glacial or

early postglacial in origin. Dating of sediments above and below this transition may establish the age offset between LU2 and LU3, which based on the sub-bottom stratigraphy must be unconformable.

EL17-IGV04-4-PC01

This core was collected from the basin between the eastern and western bedrock outcrops. The sub-bottom data reveals continuous, acoustically laminated and conformable reflectors at the coring site. However, this core is also capped by a thin layer of sand (<5 cm) (LU1) that fines downcore into a sandy silt and silt in the upper 10 cm. LU1 is not as pronounced in the MSCL data as in the other cores where it was thicker and coarser in nature. The rest of the core is composed of moderate density (1.3-1.4 g/cm³) and low susceptibility (<10 SI x10⁻⁵) sediments assigned to LU2. Slightly elevated Bd and higher and more variable Ms below 300 cm core depth corresponds to the lithologic transition towards more pronounced laminations and a greying of the sediments (Fig. 32).

EL17-IGV04-5-GC01

5-GC01 was positioned on the same sub-bottom line as 4-PC01, and located slightly to the south, where acoustic reflectors were truncated along a shallow slope, and older sediments appeared to be outcropping near the seafloor (Figs. 29 and 30). The core was capped by 1 cm thick loose sand deposit (LU1). Below this, the LU2 sediments have low to moderate density (1.3-1.4 g/cm³) and low susceptibility (<10 SI x10⁻⁵). Below 200 cm core depth, lithologic changes become more pronounced and a relatively abrupt transition into LU3 sediments occurs. These are interpreted to be correlative to the older sub-bottom reflectors that are outcropping in the area, and were not sampled by 4-PC01 (Figure 30). The LU3 sediments are more dense (1.4-1.6 g/cm³) and exhibit 2 intervals (2.26-3.08 mbsf and 4.6-5.0 mbsf) of high (>30 SI x10⁻⁵) magnetic susceptibility that appear to correlate with coarser grained and clast bearing intervals in the visual core descriptions.(Figure. 32). The LU3 sediments in 5-GC01 are highly deformed, especially near the upper contact to LU2. They appear to be laminated glacial to post-glacial clays, but the cause of their deformation is not yet clear.

Summary and future work

A key feature of the marine mapping and sub-bottom data from the survey area are numerous bedforms indicative of current activity, observations from sub-bottom data of truncated acoustic reflectors and accumulations of mounded sediment deposits that together indicate erosion and re-deposition of sediments by bottom water currents. Estimates of the northward flowing bottom water velocity in Understen-Märket trench range from 0.14 – 0.98 ms⁻¹ (Hietala et al., 2007), which lies within the predicted range of current velocities needed to dynamically sort and erode deep sea sediments (McCave and Hall, 2006). A preliminary assessment of the marine sediment cores showed that many are capped by an up to 50 cm thick coarser-grained unit, likely reflecting a current winnowed deposit overlying older delglacial and Holocene sediments. A critical implication of this is that modern deep-water advection, capable of eroding fine material from surface sediments, was not active through the entire Holocene. However we do not know when and how

this modern circulation system developed, or whether its onset was driven by climatic changes or related to post-glacial uplift.

An MSc project currently underway at IGV is utilizing the bathymetry, backscatter, sub-bottom and sediments cores to unravel how the inflow of saline waters into the Bothnian sea influences and is guided by the marine geology of Södra Kvarnen. Additionally, the project will aim to determine the timing and decipher the mechanisms that led to the advection of Baltic deep-waters into the Bothnian Sea following deglaciation.

A further outcome of this work will be the ability to age-calibrate the regional sub-bottom data, providing a framework for interpreting the timing and distribution of mass transport deposits. Based on the current collection of mapping and coring data, there does not appear to be evidence for recent mass wasting in the survey area. However this needs to be further explored in future work.

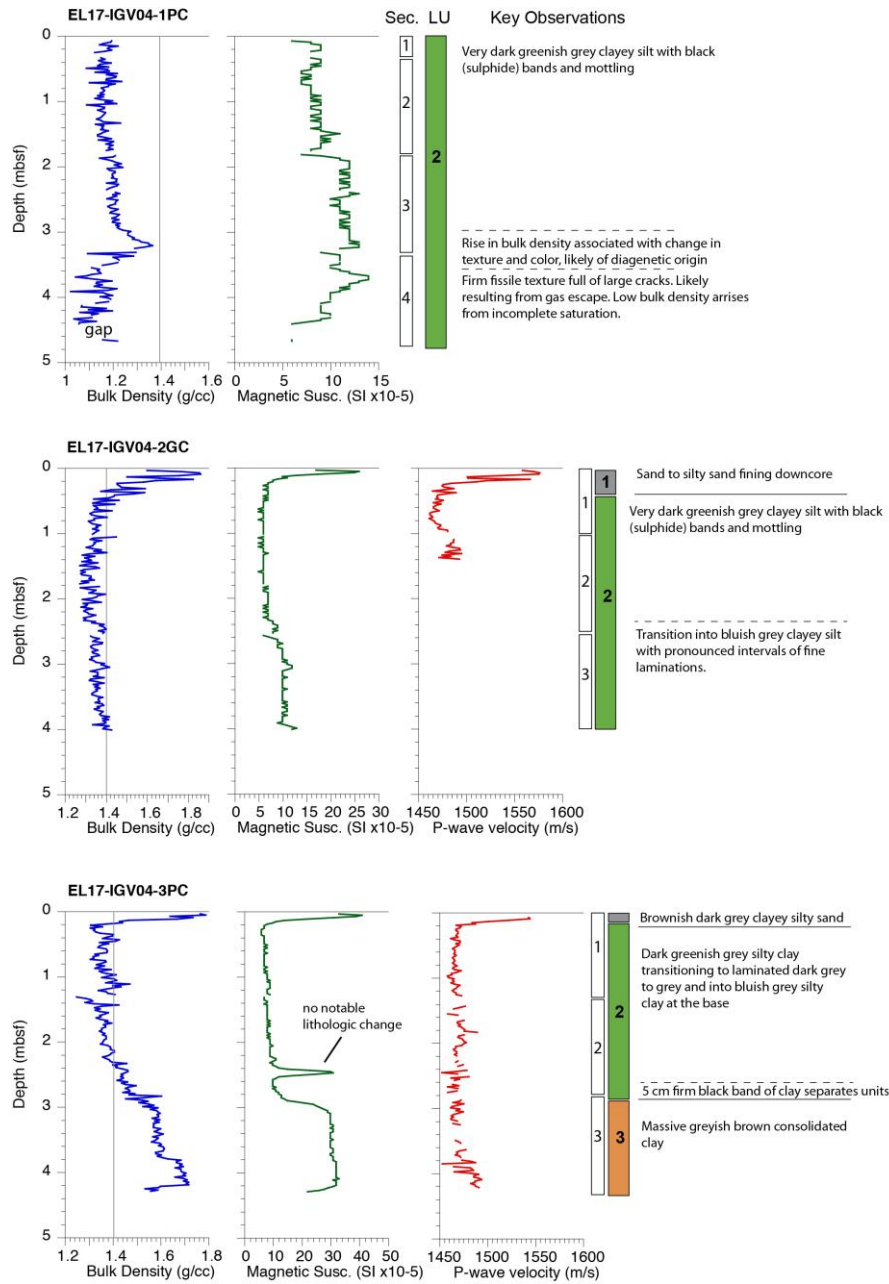


Figure 31. Integrated Multi-sensor core logging data lithologic descriptions for cores EL14-IGV04-01-PC01/02-GC01/03-PC01.

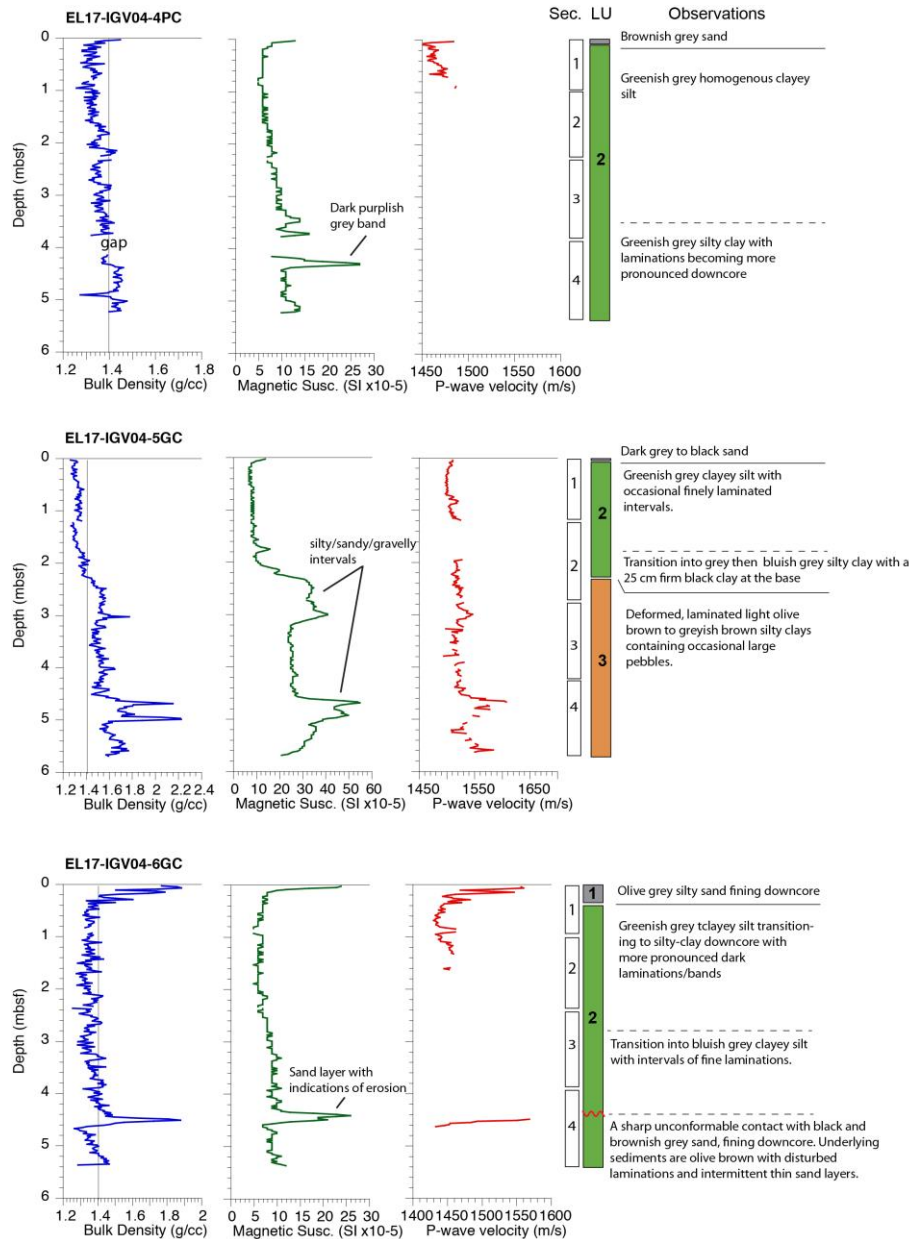


Figure 32. Integrated Multi-sensor core logging data lithologic descriptions for cores EL14-IGV04-04-PC01/05-GC01/06-GC01.

6.2.2. Temperature logging

In-situ temperature data was retrieved from 5 of the 6 cores. During the first attempt on EL17-IGV04-01-PC01, all but one of the sensors failed to connect to the programming station after deployment. After this, we were only able to find 3 remaining temperature sensors that were operating properly, and these were then deployed on the remaining 5 cores (Fig. 30). Initial evaluation of the tilt data shipboard suggests that it was negligible in all cases, $<2^\circ$ (Table 4).

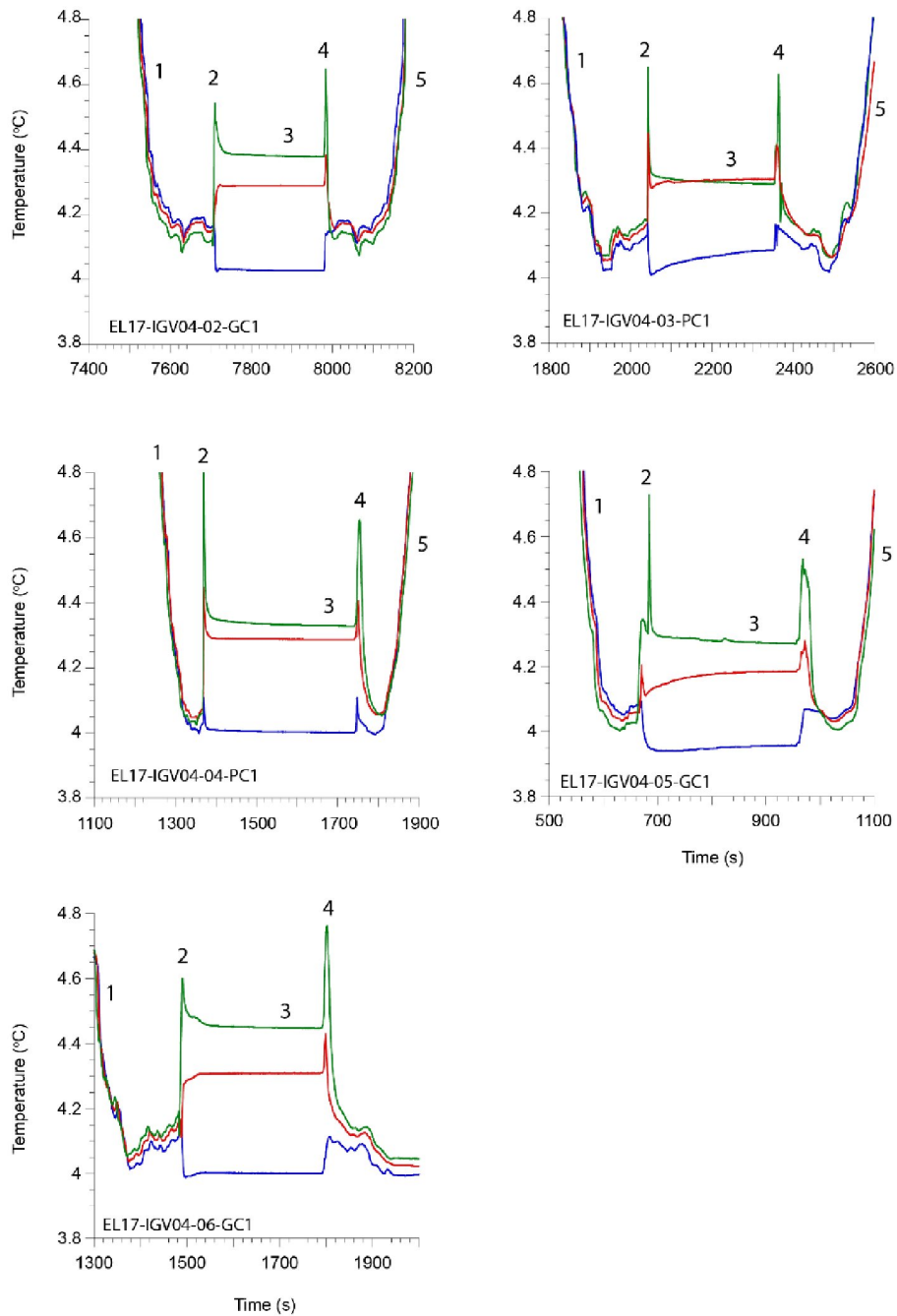


Figure 30. Temperature versus time profiles for each of the 3 sensors for successful coring deployments. The blue line is the shallowest sensor (closest to the core head) the red line the middle sensor, and the green line the deepest sensor positioned above the nose cone of the core barrel. Time, in seconds, indicates the time since the logging started. The numbers indicate stages of the core deployment and in-situ temperature measurements. 1) lowering through the water column, 2) penetration of the core into the sediments and frictional warming, 3) 5 minute period where the sensors equilibrate to ambient temperatures, 4) Frictional warming during pull-out of the coring tool from the sediments. And 5) raising the core through the water column.

To calculate accurate geothermal gradients, the temperature data would need further processing, to account for the tilt, and any offsets in the accuracy of the temperature sensors. These can be accounted for by normalizing the sensor

response to the average water column temperature recorded by all sensors (O'Regan et al., 2016). However, on 3 of the deployments (EL17-IGV04-02-GC1, EL17-IGV04-05-GC1 and EL17-IGV04-06-GC1), the in-situ temperature of the shallowest sensor is lower than the seafloor temperature. This strongly suggests that seasonal changes in bottom water temperature are influencing the geothermal gradient in the upper few meters below the seafloor, and that it is highly non-linear. Therefore, the existing in-situ measurements cannot be used to determine the true geothermal gradient, or the heat flow, without considerable data processing and modelling.

Table 4. Summary of temperature and tilt data recorded during coring operations.

Core	Tilt (°)	Sensor ID	Distance below core head (m)	Raw Temperature before pull-out (°C)
EL17-IGV04-02-GC01	1.7	1854517C	1.56	4.03
		1854515C	3.23	4.29
		1854475C	5.97	4.38
EL17-IGV04-03-PC01	1.8	1854475C	1.76	4.09
		1854515C	3.42	4.30
		1854517C	6.15	4.29
EL17-IGV04-04-PC01	1.2	1854475C	1.76	4.00
		1854517C	3.42	4.29
		1854515C	6.15	4.33
EL17-IGV04-05-GC01	0.1	1854517C	1.56	3.96
		1854515C	3.23	4.19
		1854475C	5.97	4.27
EL17-IGV04-06-GC01	0.4	1854475C	1.56	4.00
		1854515C	3.23	4.31
		1854517C	5.97	4.45

7. Results - Geophysical mapping in Swedish Lapland

One criteria for site selection of the four glaciers was that they should have old and long documentation or showing divergent response to changes in climate like differences in recession speed. By adding information on thermal structure (gained from radar), detailed mapping of the fore fields by drones and quantitative information on volume changes by photogrammetry, and glacier bed topography we retrieve paleo climate data. Some of the geo referenced models from this study can be seen at <https://sketchfab.com/ErikSH>. This compilation is made by Erik S. Holmlund. Field campaigns have been performed during the summers 2017-2019 with

field surveys and aerial photography. One radar mission was carried out in April 2017 when the lower part of Mårmaglaciären and Mårmapakteglaciären both were sounded.

Table 5. Data on the four glaciers from the airborne study. The estimation of annual mass turn-over is based on data from the 1990s until present. For Mikkaglaciären it is the net accumulation above the average transient snowline taken from aerial and satellite data and a net balance gradient of 1 m/100 m. On the other glaciers it is the net accumulation based on field surveys during years with a balanced budget.

Glacier	Volume 1990/-92 $\times 10^6 \text{ m}^3$	Volume 2008 $\times 10^6 \text{ m}^3$	Volume 2017/-18 $\times 10^6 \text{ m}^3$	Total volume change %	Annual mass turnover %
Storglaciären	310 (1992)	308	279	-10	0.67
Mikkaglaciären	550 (1990)	494	426	-23	0.58
Mårmaglaciären	440 (1991)	404	376	-15	0.15
Rabots glacier	336 (1991)	299	248	-26	0.46

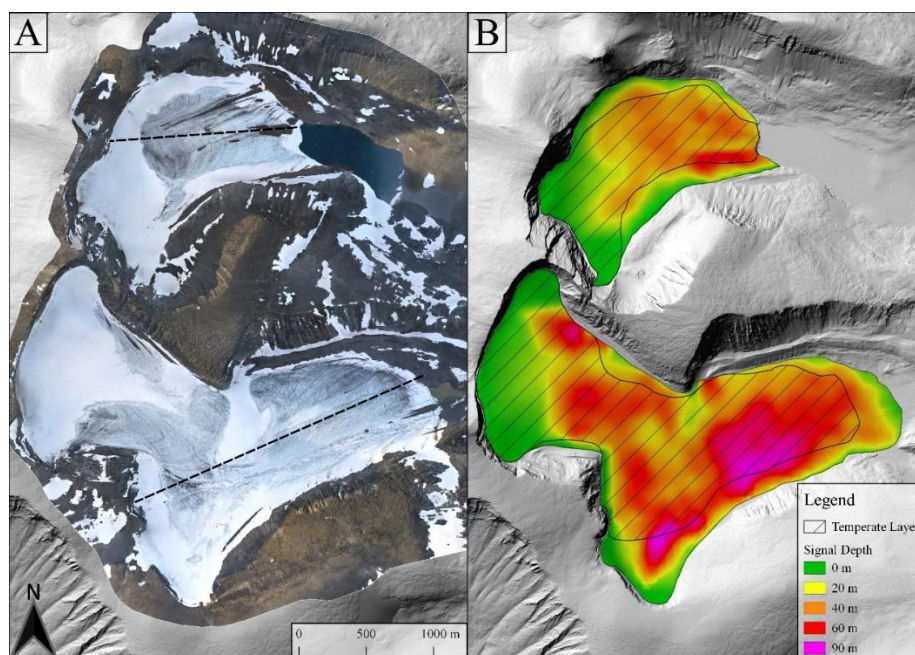


Figure 33. Results of radar survey on April 7, 2017(B) and a photogrammetric survey on August 18 (A) the same year showing the thermal conditions in Mårmaglaciären and Mårmapakteglaciären (below). In figure B the area where the glacier bottom is at its melting point is shaded and the colors indicate thickness of the below freezing part of the ice..

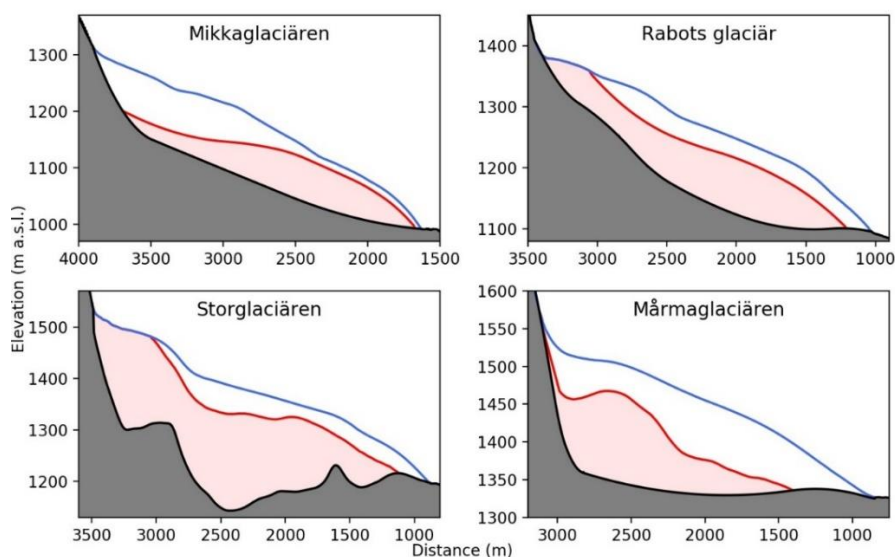


Figure 34. Bed topography and thermal conditions of the four glaciers. The bed was mapped using an 8 MHz radar. Red line indicate transition between cold and temperate ice mapped with a 900 MHz radar system. Data from this project and previous SSM-financed projects (Holmlund et al. 2016).

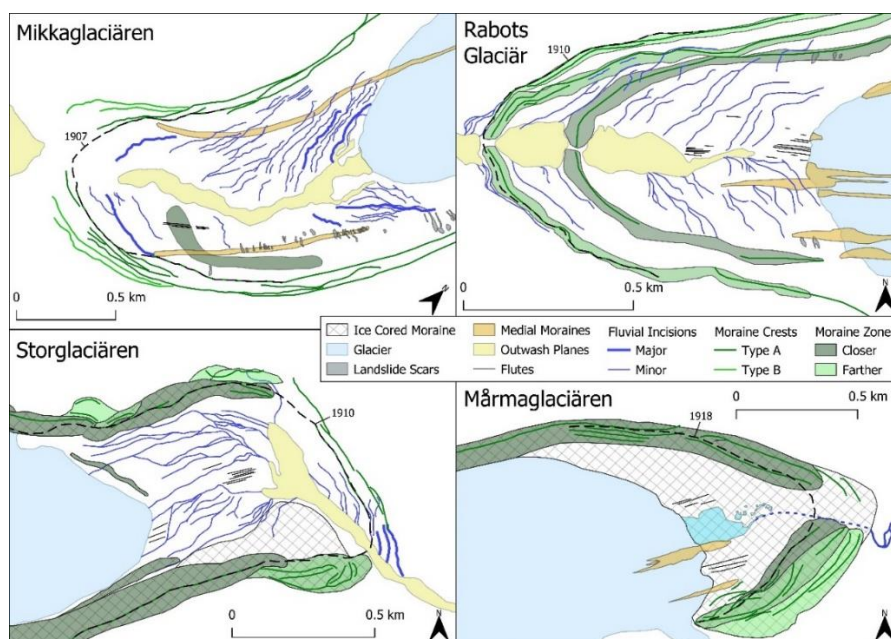


Figure 35. Geomorphologic maps constructed from Ortophotos. Drone and helicopter data from 2017 and 2018. Landforms were mapped in QGIS using the orthomosaics and DEM-derived hill shades and slope maps, created from PhotoScan. Field-checks were only done at Storglaciären, due to the lack of time at the other glaciers, and landform interpretations had to be done solely from the drone surveys and from historic images. However, the field check at Storglaciären did not change the result from the mapping based on Ortophotos so we felt convinced that our results are reliable. Not that the scale is not consistent in all figures.

In a future perspective we would like to add another 15 glaciers where sufficient background data is available. These glaciers are all recognized. We

have Kårsaglaciären in the Abisko area; Mårmapakteglaciären, E. and W. Påssusjietna, and Kåtotjkkaglaciären. In Northern Kebnekaise; Isfallsglaciären, Tarfalaglaciären, Björlings glaciär and S.Ö. Kaskasatjåkkaglaciären in the Central Kebnekaise area; Hyllglaciären, Suottasjekna, Ruotesglaciären, and Pårteglaciären in Sarek and finally Salajekna and Stuurrajekna in the Sulitelma area.

In addition to the results themselves the models we are producing are extremely powerful tools for expressing ongoing climate change. The future plan is to have a website at the Bolin centre database where models and results will be presented and we will develop a concept with virtual excursions to the glaciers. Material from this project has also been used in a book about glaciers and when and why scientists came to the Tarfala valley in Northern Sweden beginning in late 1800s. The book was published by Votum&Gullers in the spring 2020 (Holmlund and Schytt 2020).

8. Discussion and recommendation for further study

In this project we have carried out fieldwork offshore between Uppland and Åland and in the inland of Swedish Lapland to improve our understanding of the effect of a glaciation on the landscape. We have focused on the consequences of temperature distribution within the ice and the effect of changes in ice overburden pressure. The latter as a releaser of tectonic events such as earthquakes and mass wasting as has been observed elsewhere in Sweden (Jakobsson et al., 2014; Lagerbäck & Sundh, 2008). Lagerbäck et al. (2005) also made an investigation of traces of late- or postglacial faulting in the Forsmark area. It was a stratigraphic study and they found no evidences of any large earthquake, but several locations with distorted sequences of glacial clay interpreted to be caused by sliding. Hall et al. (2020) describes cracking and ripped rocks called glacially disrupted terrain in the Forsmark area. Instead of tectonic events they propose a break-up process with over pressurized groundwater beneath the ice (Hall et al. 2019, 2020). They also made estimations of the total glacial erosion in the area based on divergent elevations compared to an estimated sub-Cambrian unconformity surface and suggest some tens of metres for the last million years (Hall et al. 2019).

In the Southern Quark area, located between Uppland and the Åland archipelago, a Baltic ice stream is proposed to have existed during parts of the Weichselian glaciation, based on both submarine landforms and theoretical arguments (Greenwood et al., 2017; Holmlund and Fastook 1993). Modelling experiments suggest that the ice sheet may have been frozen to its base over Åland during the deglaciation (Holmlund and Fastook 1993). This area must have comprised a “bottle neck” for this ice stream considering that the Southern Quark forms a deep rather narrow passage between Åland and the Swedish mainland with a rough seafloor topography (Jakobsson et al., 2020). Our surveys in this project on land and in the marine realm confirm previous notions of substantial glacial activity in this area and reveal numerous new evidences of severe modulation of the landscape, e.g. mass wasting and conspicuous seafloor features.

The fieldwork in the Southern Quark included collection of sediment cores, temperature measurements in the uppermost sediments, oceanographic stations and geophysical mapping of the seafloor and upper sediment stratigraphy. In addition, acoustic measurements of the water column were acquired with RV *Electra's* fish echo sounder to investigate the occurrence of gas seep from the seabed and layers in the water.

During our pre-study of the Southern Quark (Holmlund et al. 2016), signs of mass movements were indicated in the bathymetric data provided by the Swedish Maritime Administration. The additional geophysical mapping with RV *Electra* carried out in this project provided much more details, for example, we could characterize the large rock slide in the northern part of the surveyed area that was hinted in the pre-study (Fig. 21). The mass wasted rock debris affects an area >400 m wide of the seafloor in front of the steep wall that gave away. Rock slides on land occur regularly as a consequence of long-term rock disintegration from, for example, fluvial weathering on rather steep slopes (Abele, 1994). In the submarine environment, mass movements of sediments are common and may be triggered by mechanisms such as, for example, high sedimentation rates, glacial erosion, sea-level change and tectonic movements (Leynaud et al., 2009). The occurrence of submarine rock slides is, however, much less documented and therefore also less known. A geohazard from large mass movements on the seafloor, whether of rocks or sediments, is the generation of a tsunami (Ioualalen et al., 2010). A numerical simulation of a potential tsunami caused by the identified rock slide in the Southern Quark comprises one of several topics for follow-up studies that could be made based on the material acquired in this study, as it may have bearing on storage of nuclear waste in the Forsmark area.

A conspicuous channel with sharp bents was mapped in the northern part of the surveyed area of the Southern Quark (Fig. 22). Its appearance opens for the possibility that it could have been initiated by downfolding of the upper sediment layers due to movements in the bedrock below and thus indicate postglacial movements. The bathymetric expression of the channel is to some extent similar to features previously mapped in Lake Vättern, Southern Sweden (Jakobsson et al., 2014). In Lake Vättern, structures formed in the sediment stratigraphy were interpreted to be caused by postglacial tectonic vertical displaced of as much as 13 m, over a stretch of > 80 km, in the bedrock underlying the unconsolidated sediments. Here in the Southern Quark, we find the conspicuous channel in a small area of 1500 x 500 m and its maximum depth is 6 m. It may be formed by bottom currents. Additional acquisition of high-resolution geophysical mapping data, in particular sub-bottom profiles across the feature at several locations, may resolve its nature. Further analyses of the retrieved sediment cores may also provide some age constraints of the rock slide as well as the channel, although for a precise dating new more strategically located sediment cores will have to be collected.

In general, the survey of the area shows strong bottom currents and a very dynamic oceanography in the area today. Beneath the top sediment layers are buried channels that are probably derived from deglaciation and a plentiful supply of melt water.

The studies in Swedish Lapland concerned how the temperature distribution within the ice determine landscape formation. A number of well-studied retreating glaciers were chosen. By executing radar sounding, the thermal structure was mapped and the landforms in the pro glacial area were mapped by using photogrammetry based on photographs taken from helicopter and drones. The results show clearly the effect of the thermal conditions and they also show both that the boundary between basal frozen and basal melting conditions is sharp and it may move its position over time due to changes in ice thickness and climate change. In an analogue to basal conditions beneath the Weichselian ice sheet there may have been short distances between high erosion rates and hardly no erosion at all. The transition zone between these two different environments is not stable over time and is rather expected to have varied in its location.

9. Conclusions

- Mass wasted rock debris on the seafloor is mapped in the Southern Quark, between mainland of Sweden and Åland, at the base of a steep ridge. The mass wasted material occurs over a >400 m wide area and originates from the submarine ridge's wall that collapsed.
- Determining the time of the mass-wasting event may be possible if we are able to age-calibrate the sub-bottom stratigraphy using existing sediment cores.
- The mass-wasting event may have triggered a tsunami. Follow-up studies involving numerical tsunami-simulations could test this hypothesis as the critical required input parameters can be provided from this study.
- Mapped sharp folds in the uppermost soft sediment may indicate post-glacial tectonic activity in the Southern Quark area.
- Much of the seafloor in the Southern Quark area appears to be heavily influenced by modern bottom-water currents. Sediment cores suggest that this circulation system was not active during the entire Holocene. Current work aims to document the onset of this circulation system and establish its connection to regional climate change and/or post-glacial rebound in the Bothnian Basin.
- Seafloor channels buried below the uppermost sediments suggest a glacial environment characterized by a rich supply of meltwater.
- The survey on alpine glaciers in northern Sweden shows that the spatial transition between basal frozen and basal melting varies over time. Changes in ice thickness, climate or heat generated by internal deformation alter the position of the transition zone. In a glaciation the duration of the cold period is also of importance for the basal conditions.
- The temperature distribution within a glacier governs ice flow pattern, landform formation and erosion rate.

- Though there are no surges observed in Sweden several glaciers full-fill the physical criteria to become a surging glacier in a colder climate.

References

- Abele, G., 1994, Large Rockslides: Their causes and movement on internal sliding planes: *Mountain research and Development*, v. 14, no. 4, p. 315-320.
- Alexandersson, H. and Eriksson, B., 1987: *Climate Fluctuations in Sweden 1860-1987*. Swedish Meteorological and Hydrological Institute (SMHI), RMK 58, 54 pp.
- Andrén, T., Barker Jørgensen, B., Cotterill, C., Green, S., and the I. e. s. p., 2015, IODP expedition 347: Baltic Sea basin paleoenvironment and biosphere: *Scientific Drilling*, v. 20, p. 1-12.
- Andrén, T., Björck, S., Andrén, E., Conley, D., Zillén, L., and Anjar, J., 2011, The Development of the Baltic Sea Basin During the Last 130 ka, *in* Harff, J., Björck, S., and Hoth, P., eds., *The Baltic Sea Basin: Berlin, Heidelberg, Springer Berlin Heidelberg*, p. 75-97.
- Beckholmen, M., and Tirén., S. A., 2009, The geological history of the Baltic Sea: A review of the literature and investigation tools. *SSM report 2009:21*.
- Björck, S., 1995, A review of the history of the Baltic Sea, 13.0-8.0 ka BP: *Quaternary International*, v. 27, p. 19-40.
- Dowdeswell, J. A., Canals, M., Jakobsson, M., Todd, B. J., Dowdeswell, E. K., & Hogan, K. A. (2016). The variety and distribution of submarine glacial landforms and implications for ice-sheet reconstruction. *Geological Society, London, Memoirs*, 46(1), 519-552. <http://mem.lyellcollection.org/content/46/1/519.short>
- Dowdeswell, J.A., Hodkins, R., Nuttall, A.M., Hagen, J.O., Hamilton, G.S., 1995, Mass balance change as a control on the frequency and occurrence of glacier surges in Svalbard, Norwegian High Arctic. *Geophysical Research Letters* 22: 2909-2912. Doi: 10.1029/95GL02821.
- Ehlers, J., Gibbard, P. L., & Hughes, P. D. (2018). Chapter 4 - Quaternary Glaciations and Chronology. In J. Menzies & J. J. M. van der Meer (Eds.), *Past Glacial Environments (Second Edition)* (pp. 77-101): Elsevier.
- Farnsworth, W.R., Ingólfsson, Ó., Retelle, M., Schomacher, A., 2016, Over 400 previously undocumented Svalbard surge-type glaciers identified. *Geomorphology*, v. 264, p. 52-60. Doi: 10.1016/j.geomorph.2016.03.025.
- Flodén, T., 1992, Östersjöns geologiska utveckling, *in* Kullinger, B., ed., *Östersjön - ett hav i förändring*, Naturvetenskapliga forskningsrådet, p. 9-20.
- Flodén, T., Jacobsson, R., Kumpas, M. G., Wadstein, P., and Wannäs, K., 1980, Geophysical investigation of western bothnian bay: *GFF*, v. 101, no. 4, p. 321-327.

- Greenwood, S. L., Clason, C. C., and Jakobsson, M., 2016a, Ice-flow and meltwater landform assemblages in the Gulf of Bothnia: Geological Society, London, *Memoirs*, v. 46, no. 1, p. 321-324.
- Greenwood, S. L., Clason, C. C., Nyberg, J., Jakobsson, M., and Holmlund, P., 2017, The Bothnian Sea ice stream: early Holocene retreat dynamics of the south-central Fennoscandian Ice Sheet: *Boreas*, v. 46, no. 2, p. 346-362. <http://dx.doi.org/10.1111/bor.12217>
- Greenwood, S. L., Jakobsson, M., Hell, B., and Öiås, H., 2016b, Esker systems in the Gulf of Bothnia: Geological Society, London, *Memoirs*, v. 46, no. 1, p. 209-210.
- Hall, A. M., Krabbendam, M., Boeckel, van M., Ebert, K., Hättestrand, C., Heyman, J., 2019: The sub-Cambrian unconformity in Västergötland, Sweden: Reference surface for Pleistocene glacial erosion of basement. *SKB TR-19-21*, Svensk Kärnbränslehantering AB. <https://www.skb.com/publication/2495096>
- Hall, A. M., Krabbendam, M., Boeckel, van M., Bradley, W., Hättestrand, C., Heyman, J., Palamakumbura, R.N., Stroeven, A.P. and Näslund, J-O., 2020: Glacial ripping: geomorphological evidence from Sweden for a new process of glacial erosion, *Geografiska Annaler: Series A, Physical Geography*, DOI: [10.1080/04353676.2020.1774244](https://doi.org/10.1080/04353676.2020.1774244)
- Holmlund, P., 1993, Surveys of Post-Little Ice Age glacier fluctuations in northern Sweden. *Zeitschrift für Gletscherkunde und Glazialgeologie* V. 29, no. 1, p. 1-13.
- Holmlund, P., 1998, Glaciers as detailed climatic records in subpolar environments: *Ambio* v.4, p. 266-269.
- Holmlund, E.S., 2020: Rapid temperature rise may have triggered glacier surges all over Svalbard. Master thesis in geology, Department of Geosciences, University of Tromsø (UiT), 56 pp.
- Holmlund, P. and Eriksson, M. 1989, The cold surface layer on Storglaciären: *Geografiska Annaler*, v. 71A, no 3–4, p. 241–244.
- Holmlund, P. and Schytt, A., 2020: *Glaciärerna i Kebnekaise – från lilla istiden till dagens klimatuppvärmning*. (ISBN 978-91-89021-05-1), Votum förlag, 136 pp.
- Holmlund, P., Clason, C., Blomdahl, K., 2016, The effect of a glaciation on East Central Sweden: case studies on present glaciers and analyses of landform data. Technical Report 2016:21. Strålsäkerhetsmyndigheten.
- Holmlund, P., Fastook, J., 1993: Numerical modelling provides evidence of a Baltic ice stream during the Younger Dryas. *Boreas* 22 (2): 77-86.
- Holmlund, P., Holmlund, E.S., 2018, Recent climate-induced shape changes of the summit of Kebnekaise, Northern Sweden: *Geografiska Annaler, series A, Physical Geography*, doi.org/10.1080/04353676.2018. 1542130.
- Holmlund, E.S., Holmlund, P., 2019, Constraining 135 Years of Mass balance with Historic Structure-from-Motion Photogrammetry on Storglaciären, Sweden: *Geografiska Annaler, Series A, Physical Geography* doi: 10.1080/04353676.2019.1588543.
- Hughes, A. L. C., Gyllencreutz, R., Lohne, Ø. S., Mangerud, J., & Svendsen, J. I. (2016). The last Eurasian ice sheets – a chronological database

- and time-slice reconstruction, DATED-1. *Boreas*, 45(1), 1-45.
<http://dx.doi.org/10.1111/bor.12142>
- Ioualalen, M., Migeon, S., and Sardoux, O., 2010, Landslide tsunami vulnerability in the Ligurian Sea: case study of the 1979 October 16 Nice international airport submarine landslide and of identified geological mass failures: *Geophysical Journal International*, v. 181, no. 2, p. 724-740. Doi: 10.1111/j.1365-246X.2010.04572.x
- Jakobsson, M., Björck, S., O'Regan, M., Flodén, T., Greenwood, S. L., Swärd, H., et al. (2014). Major earthquake at the Pleistocene-Holocene transition in Lake Vättern, southern Sweden. *Geology*, 42(5), 379-382.
<http://geology.gsapubs.org/content/early/2014/03/17/G35499.1.abstract>
- Jakobsson, M., Stranne, C., O'Regan, M., Greenwood, S.L., Gustafsson, B., Humborg, C., and Weidner, E., 2019, Bathymetric properties of the Baltic Sea: *Ocean Science*, v. 15, no. 4, p. 905-924, doi:10.5194/os-15-905-2019. <https://www.ocean-sci.net/15/905/2019/>
- Jakobsson, M., Greenwood, S. L., Hell, B., and Öiås, H., 2016, Drumlins in the Gulf of Bothnia: *Geological Society, London, Memoirs*, v. 46, no. 1, p. 197-198.
- Kleman, J., Hättstrand, C., Borgström, I., and Stroeven, A., 1997, Fennoscandian palaeoglaciology reconstructed using a glacial geological inversion model: *Journal of Glaciology*, v. 43, no. 144, p. 283-299.
- Lagerbäck, R., Sundh, M., Svedlund, J-O. and Johansson, H., 2005: Forsmark site investigation. Searching for evidence of late- or postglacial faulting in the Forsmark region. Results from 2002-2004. Svensk Kärnbränslehantering AB, ISSN 1402-3091. SKB Rapport R-05-51, 50 pp.
- Lagerbäck, R., & Sundh, M. (2008). *Early Holocene faulting and paleoseismicity in northern Sweden*. Sveriges geologiska undersökning (ISBN 978-91-7158-859-3), Research paper C836, 80p. <http://resource.sgu.se/produkter/c/c836-rapport.pdf>
- Lemieux, J.-M., & Sudicky, E. A. (2011). Glaciations and Groundwater Flow Systems. In V. P. Singh, P. Singh, & U. K. Haritashya (Eds.), *Encyclopedia of Snow, Ice and Glaciers* (pp. 372-376). Dordrecht: Springer Netherlands.
- Leynaud, D., Mienert, J., and Vanneste, M., 2009, Submarine mass movements on glaciated and non-glaciated European continental margins: A review of triggering mechanisms and preconditions to failure: *Marine and Petroleum Geology*, v. 26, no. 5, p. 618-632. Doi: 10.1016/j.marpetgeo.2008.02.008
- Lundqvist, J., 2004, Glacial history of Sweden, in Ehlers, J., and Gibbard, P. L., eds., *Developments in Quaternary Sciences, Volume Volume 2, Part 1*, Elsevier, p. 401-412.
- , 2007, Surging ice and break-down of an ice dome – a deglaciation model for the Gulf of Bothnia: *GFF*, v. 129, no. 4, p. 329-336.
- Midgley, N., Tonkin, T., 2017, Reconstruction of former glacier surface topography from archive oblique aerial images: *Geomorphology*, v. 282, p. 18-26. Doi: 10.1016/j.geomorph.2017.01.008.

- O'Regan, M., Preto, P., Stranne, C., Jakobsson, M., and Koshurnikov, A., 2016, Surface heat flow measurements from the East Siberian continental slope and southern Lomonosov Ridge, Arctic Ocean: *Geochemistry, Geophysics, Geosystems*, v. 17, no. 5, p. 1608-1622. 10.1016/j.geomorph.2017.01.008.
- Pettersson, R., P. Jansson, H. Huwald, H. Blatter (2007). Spatial pattern and stability of the cold surface layer on Storglaciären, Sweden. *Journal of Glaciology*, v. 53, p. 99-109
- Pfender, M., and Villinger, H., 2002, Miniaturized data loggers for deep sea sediment temperature gradient measurements: *Marine Geology*, v. 186, no. 3, p. 557-570.
- Raymond, C.F., 1987: How do glaciers surge? A review. *Journal of Geophysical Research* 92:9121. Doi: 10.1029/JB092iB09p09121.
- Sevestre, H., Benn, D.I., 2015: Climatic and geometric controls on the global distribution of surge-type glaciers: implications for unifying model of surging: *Journal of Glaciology*, v. 61, p. 646-662. Doi: 10.3189/2015JoG14J136.
- Steffen, R., Wu, P., Steffen, H., & Eaton, D. W. (2014). The effect of earth rheology and ice-sheet size on fault slip and magnitude of postglacial earthquakes. *Earth and Planetary Science Letters*, 388(0), 71-80.
<http://www.sciencedirect.com/science/article/pii/S0012821X13007036>
- Tuuling, I., Flodén, T., and Sjöberg, J., 1997, Seismic correlation of the Cambrian sequence between Gotland and Hiiumaa in the Baltic Sea: *GFF*, v. 119, no. 1, p. 45-54.
- Winterhalter, B., Flodén, T., Ignatius, H., Axberg, S., and Niemistö, L., 1981, Chapter 1 Geology of the Baltic Sea: Elsevier Oceanography Series v. 30, p. 1-121.

Appendix 1: deliverables

Holmlund, P., Holmlund, E.S., 2018: Recent climate-induced shape changes of the summit of Kebnekaise, Northern Sweden. *Geografiska Annaler, series A, Physical Geography*, doi.org/10.1080/04353676.2018.1542130.

Holmlund, P., Holmlund, E.S., 2018: New methods make use of old photographs and allow quantitative analyses of glacier changes. Poster presentation at the EGU-meeting in Vienna, April 2018.

Holmlund, E.S., Holmlund, P., 2019: Constraining 135 Years of Mass balance with Historic Structure-from-Motion Photogrammetry on Storglaciären, Sweden. *Geografiska Annaler, Series A, Physical Geography* doi: 10.1080/04353676.2019.1588543.

Jakobsson, M., C. Stranne, M. O'Regan, S. L. Greenwood, B. Gustafsson, C. Humborg, and E. Weidner (2019), Bathymetric properties of the Baltic Sea, *Ocean Science*, v. 15, no. 4, p. 905-924, doi:10.5194/os-15-905-2019.

Stranne, C., 2019: Acoustic EK80 midwater data, published in the Bolin Centre data base: <https://bolin.su.se/data/jakobsson-2019-2>

Jakobsson, M., 2019: Multibeam and sub-bottom profiles to be published in the Bolin Centre data base.

Wagner, A.. in prep. Marine Geology and Holocene Paleoceanography of Södra Kvarken, Baltic Sea. 60 hp thesis in Master of Science, IGV, Stockholm University.

Jakobsson, M., et al. in prep, Mass wasting and bottom current features in the connection between the Bothnian Sea and Northern Baltic Proper. Planned to be ready for submission during fall of 2022.

Holmlund, P., Holmlund, E.S., 2019: The impact of internal thermal regime of glaciers on climate caused advance and retreat. Poster presentation at the IUGG/IACS meeting in Montreal July 10-18.

Holmlund, P., Mannerfelt, E.S., In prep.: Polythermal Glacier Advance Dynamics in Sweden. It will be two papers entirely based on data from this project and both will hopefully be published during 2022.

Appendix 2: Core Logs

Station	Type JPC/PC/ GC/TWC	Latitude North	Longitude West/East	Water Depth (m)	Core Head Weight (kg)	Trigger Weight (kg)	Free Fall Length (m)	Rigged Length (m)	Liner Type
EL17-IGV-01-PC1	PC/TWC	60d 21.1758'	18d 58.9081'	180	472	3 small, 1 large	2.0	6	PVC
	Core Catcher	Pull Out	Core on Bottom yymmdd	Core on Bottom Shiptime	Core on Bottom UTC	Penetration (m)			
	Type	Force (kg)							
	Finger		170815	11:58	9:58	Up on weights			
Section	Length (m)	Recovery (m)	Comments						
1 G	0.27	0.2	In water: 09:54 UTC, 11:54 Local. Out of water: 10:15 UTC, 12:15 Local time. Trigger weight core 46 cm, stored as EL17-IGV04-01TWC. 177m water dept logged on winch when trigging. Left in for 5 minutes to log temp data from 3 sensors.						
2 F-E	1.5	1.5							
3 D-C	1.5	1.5							
4 B-A	1.5	1.5							
5									
6									
7									
8									
Core Catcher	0	0							
Total Core	4.77	4.7							
Station	Type JPC/PC/ GC/TWC	Latitude North	Longitude West/East	Water Depth (m)	Core Head Weight (kg)	Trigger Weight (kg)	Free Fall Length (m)	Rigged Length (m)	Liner Type
EL17-IGV-02-GC1	GC	60d 20.8447'	18d 57.046'	202	472	NA	NA	6	PVC
	Core Catcher	Pull Out	Core on Bottom yymmdd	Core on Bottom Shiptime	Core on Bottom UTC	Penetration (m)			
	Type	Force (kg)							
	Finger		170815	15:59	13:59	below core head			
Section	Length (m)	Recovery (m)	Comments						
1 G	1	1	>12 m/s, rough sea. For this reason we changed to gravity core. Gyro worked superbly and also DP. Taken west of the westerly large rotated block, along its slope near where we saw flares on EK80. Gray clay in core cutter. Olive gray clay in top.						
2 F-E	1.5	1.5							
3 D-C	1.5	1.5							
4 B-A	0	0							
5									
6									
7									
8									
Core Catcher									
Total Core	4	4							

Station	Type JPC/PC/ GC/TWC	Latitude North	Longitude West/East	Water Depth (m)	Core Head Weight (kg)	Trigger Weight (kg)	Free Fall Length (m)	Rigged Length (m)	Liner Type
EL17-IGV04-03-PC1	PC/TWC	60d 21.3757'	18d 57.6794'	207	472	3 small, 1 large	2.0	6	PVC
	Core Catcher	Pull Out	Core on Bottom	Core on Bottom	Core on Bottom	Penetration			
	Type	Force (kg)	yymmdd	Shiptime	UTC	(m)			
	Finger		170817	12:04	10:04	Up on weights			
Section	Length (m)	Recovery (m)	Comments						
1 E-F	1.5	1.5	Core in bottom for 5 min for three temp loggers. TWS 25 cm, stored as EL17-IGV04-03TWC. Core catcher not included in recovery.						
2 C-D	1.5	1.5							
3 A-B	1.29	1.27							
4	0	0							
5									
6									
7									
8									
Core Catcher	0.15	0.15							
Total Core	4.29	4.27							
Station	Type JPC/PC/ GC/TWC	Latitude North	Longitude West/East	Water Depth (m)	Core Head Weight (kg)	Trigger Weight (kg)	Free Fall Length (m)	Rigged Length (m)	Liner Type
EL17-IGV04-04-PC1	PC/TWC	60d 19.9996'	18d 57.6722'	146	472	3 small, 1 large	2.0	6	PVC
	Core Catcher	Pull Out	Core on Bottom	Core on Bottom	Core on Bottom	Penetration			
	Type	Force (kg)	yymmdd	Shiptime	UTC	(m)			
	Finger		170817	14:04:00 PM	12:04	Up on weights			
Section	Length (m)	Recovery (m)	Comments						
1 G-H	0.82	0.82	Core in bottom for 5 min for three temp loggers. TWC, stored as EL17-IGV04-04TWC. Core catcher not included in recovery.						
2 E-F	1.44	1.44							
3 C-D	1.29	1.27							
4 A-B	1.49	1.49							
5									
6									
7									
8									
Core Catcher	0.15	0.15							
Total Core	5.04	5.02							

Station	Type JPC/PC/ GC/TWC	Latitude North	Longitude West/East	Water Depth (m)	Core Head Weight (kg)	Trigger Weight (kg)	Free Fall Length (m)	Rigged Length (m)	Liner Type
EL17-IGV04-05-GC1	GC	60d 19.3446'	18d 57.6711'	149	472	Na	Na	6	PVC
	Core Catcher	Pull Out	Core on Bottom	Core on Bottom	Core on Bottom	Penetration			
	Type	Force (kg)	yymmdd	Shiptime	UTC	(m)			
	Finger		170817	13:18:00 PM	15:18:00 PM	m below weights			
Section	Length (m)	Recovery (m)	Comments						
1 G-H	1.5	1.5	Core in bottom for 5 min for three temp loggers. Penetrate to about 20 cm below weights						
2 E-F	1.49	1.49							
3 C-D	1.5	1.5							
4 A-B	1.21	1.21							
5									
6									
7									
8									
Core Catcher	0	0							
Total Core	5.7	5.7							
Station	Type JPC/PC/ GC/TWC	Latitude North	Longitude West/East	Water Depth (m)	Core Head Weight (kg)	Trigger Weight (kg)	Free Fall Length (m)	Rigged Length (m)	Liner Type
EL17-IGV04-06-GC1	GC	60d 20.784'	18d 57.0406'	197	472	Na	Na	6	PVC
	Core Catcher	Pull Out	Core on Bottom	Core on Bottom	Core on Bottom	Penetration			
	Type	Force (kg)	yymmdd	Shiptime	UTC	(m)			
	Finger		170817	16:35	14:35	m below weights			
Section	Length (m)	Recovery (m)	Comments						
1 G-H	0.86	0.86	Core in bottom for 5 min for three temp loggers. Penetrate to weights. Prepared for Rhizon sampling, every 30 cm. The winch wire skipped a loop, so the corer had to be lowered down to the seafloor again, risk for double coring in the bottom section. Must be check when opened. This core was taken where seep was observed in EK 80. Seep could not be reconfirmed during the second passage, could be intermittent.						
2 E-F	1.49	1.49							
3 C-D	1.5	1.5							
4 A-B	1.51	1.51							
5									
6									
7									
8									
Core Catcher	0	0							
Total Core	5.36	5.36							

The Swedish Radiation Safety Authority has a comprehensive responsibility to ensure that society is safe from the effects of radiation. The Authority works from the effects of radiation. The Authority works to achieve radiation safety in a number of areas: nuclear power, medical care as well as commercial products and services. The Authority also works to achieve protection from natural radiation and to increase the level of radiation safety internationally.

The Swedish Radiation Safety Authority works proactively and preventively to protect people and the environment from the harmful effects of radiation, now and in the future. The Authority issues regulations and supervises compliance, while also supporting research, providing training and information, and issuing advice. Often, activities involving radiation require licences issued by the Authority. The Swedish Radiation Safety Authority maintains emergency preparedness around the clock with the aim of limiting the aftermath of radiation accidents and the unintentional spreading of radioactive substances. The Authority participates in international co-operation in order to promote radiation safety and finances projects aiming to raise the level of radiation safety in certain Eastern European countries.

The Authority reports to the Ministry of the Environment and has around 300 employees with competencies in the fields of engineering, natural and behavioral sciences, law, economics and communications. We have received quality, environmental and working environment certification.

Publikationer utgivna av Strålsäkerhetsmyndigheten kan laddas ned via stralsakerhetsmyndigheten.se eller beställas genom att skicka e-post till registrator@ssm.se om du vill ha broschyren i alternativt format, som punktskrift eller daisy.

Strålsäkerhetsmyndigheten
Swedish Radiation Safety Authority
SE-171 16 Stockholm
Phone: 08-799 40 00
Web: ssm.se
E-mail: registrator@ssm.se

©Strålsäkerhetsmyndigheten